EURO Journal on Transportation and Logistics 11 (2022) 100090

Contents lists available at ScienceDirect

EURO Journal on Transportation and Logistics

journal homepage: www.sciencedirect.com/journal/euro-journal-on-transportation-and-logistics

A game-theoretic approach for reliability evaluation of public transportation transfers with stochastic features

Giorgio Gnecco[a], Yuval Hadas[b,*], Marcello Sanguineti[c]

[a] AXES Research Unit, IMT Alti Studi Lucca, Piazza S. Francesco, 19 - 55110, Lucca, Italy
[b] Department of Management, Bar-Ilan University, Max ve-Anna Webb street, Ramat Gan, 5290002, Israel
[c] Department of Bioengineering, Robotics, Informatics, and Systems Engineering, University of Genova, Via Opera Pia, 13 - 16145, Genova, Italy

ARTICLE INFO

Keywords:
Public transportation systems
Analysis of transfers
Transferable utility games
Stochastic transfer times
Network reliability

ABSTRACT

A game-theoretic approach based on the framework of transferable-utility cooperative games is developed to assess the reliability of transfer nodes in public transportation networks in the case of stochastic transfer times. A cooperative game is defined, whose model takes into account the public transportation system, the travel times, the transfers and the associated stochastic transfer times, and the users' demand. The transfer stops are modeled as the players of such a game, and the Shapley value – a solution concept in cooperative game theory – is used to identify their centrality and relative importance. Theoretical properties of the model are analyzed. A two-level Monte Carlo approximation of the vector of Shapley values associated with the nodes is introduced, which is efficient and able to take into account the stochastic features of the transportation network. The performance of the algorithm is investigated, together with that of its distributed computing variation. The usefulness of the proposed approach for planners and policy makers is shown with a simple example and on a case study from the public transportation network of Auckland, New Zealand.

1. Introduction

1.1. Transfers in public transportation systems

Public Transportation (*PT*) systems are expected to be an efficient, sustainable, and affordable transportation mode. The efficiency is achieved mainly by high-capacity vehicles connecting major demand generators to major destinations. A serious drawback of PT systems is the network structure, which is based mostly on fixed routes. In contrast, private cars and taxi freely traverse the road network, and provide a direct door-to-door service to the users. In order to compete with these modes, PT systems should provide better coverage, or connectivity.

One option is to add new routes, which directly connect otherwise unserved origins and destinations. However, this approach decreases efficiency (more vehicles, more distance traveled, etc.) and therefore decreases sustainability and affordability. On the other hand, it is possible to significantly increase connectivity via indirect trips, i.e., trips that require one or more transfers (e.g., alighting from one vehicle and boarding another one in order to continue the trip). This approach was termed "*the network effect*" by Mees (2010), and was demonstrated by a simple grid network, illustrated in Fig. 1 (a). If it is assumed that walking is not possible between adjacent nodes (the intersections between blocks and locations of stops), then a north-south PT network provides connectivity to 900 origin-destination pairs, or OD pairs (Fig. 1, b), i.e., 10 routes, each serving 10×9 OD pairs. As the total number of OD pairs is 9900, this results in a poor coverage (900 out of 9900). The introduction of west-east routes (Fig. 1, c) doubles the number of directly connected OD pairs. Moreover, the remaining 8100 OD pairs are indirectly connected via a single transfer (from a north-south route to a west-east route or vice versa). This corresponds to a complete network coverage.

Nevertheless, transfers could induce reliability issues as a consequence of the stochastic nature of the system. For this reason, a transfer may be missed due to a delay, causing longer travel times and frustration to the travelers. Moreover, since service reliability is a major attribute for modal shift from car to PT (Redman et al., 2013), an unreliable PT system discourages modal shift. Similar findings (Bates et al., 2001) rate reliability as a very important feature, affecting both passengers' perceptions and levels of use of the different modes.

In this work, we investigate the relative importance of transfer stops in public transportation systems with stochastic transfer times.

* Corresponding author.
E-mail addresses: giorgio.gnecco@imtlucca.it (G. Gnecco), yuval.hadas@biu.ac.il (Y. Hadas), marcello.sanguineti@unige.it (M. Sanguineti).

https://doi.org/10.1016/j.ejtl.2022.100090
Received 23 November 2021; Received in revised form 15 June 2022; Accepted 1 August 2022
Available online 13 August 2022

1.2. Literature review

Addressing transfers reliability is possible in the planning or operation phases of PT systems. For the former, PT network design can be carried on by considering travel time variability (Yao et al., 2014). As to the latter, real-time operations strategies, such as skip-stop and holding (Hadas and Ceder, 2010; Nesheli and Ceder, 2015) can be used to synchronize transfers by controlling the arrival time of vehicles at a transfer stop (i.e., expediting arrival with skip-stop, or delaying arrival with holding). However, both approaches are complex to optimize, and work well only for small-size networks. This calls for the identification of critical transfers, as part of network reliability analysis. Given a small subset of nodes (the critical transfers), the above-mentioned approaches can be more efficient for improving the PT network' reliability.

Indeed, network reliability assessment, as well as identification of vulnerability and design of resilient transportation networks, is an important topic of current research. Bell (2000) developed a model for measuring the performance reliability of transportation networks, based on link failure. The failure occurs with a given probability and causes an additional travel time. This can be related to transfer reliability, as the lack of reliability is realized by missing a transfer and by the consequent additional travel time. Vulnerability can be assessed by investigating connectivity, as suggested by Reggiani et al. (2015). The authors demonstrated therein that the concept of connectivity is well-suited to the analysis of resilience and vulnerability of transportation systems (see also Gu et al., 2020 for an overview of the definitions of reliability, vulnerability, and resilience). Furthermore, connectivity assessment should be based on quantitative measures, which can be used to rank nodes or links with respect to their importance, as proposed by Jenelius and Mattsson (2015). This approach makes it possible, for instance, to identify parts of the transportation system, for which network disruptions would be quite severe. The identification of important elements means that suitable focused countermeasures should be used to decrease the risk. Estimating criticality can be done by assessing the effect of one link closure to the overall performance of the network. To analyze urban bus service reliability, specific PT reliability measures can be computed for different components of the system, such as stops, routes, and the whole network (Chen et al., 2009).

Classical approaches to investigate network reliability and vulnerability come from the scientific literature related to the analysis of social networks (Wasserman and Faust, 1994) and cope with this issue by properly defining and investigating centrality of the network nodes. Several centrality measures were defined, like *betweenness centrality*, *closeness centrality*, and *degree centrality* (Wasserman and Faust, 1994, chapter 10). Several authors defined various ways to measure connectivity, which are applicable to general networks (Ahuja et al., 1993; Black, 2003; Rodrigue et al., 2006) and, particularly, also to transportation networks (Mishra et al., 2012) and to public transportation networks (Hadas and Ranjitkar, 2012; Hadas, 2013). Centrality measures have been used not only for road networks, but also for container shipping networks in maritime transport (Cheung et al., 2020), and for air cargo shipping networks (Bombelli et al., 2020).

As pointed out by Hadas et al. (2017) and Gnecco et al. (2021), classical measures of centrality often suffer from an intrinsic limitation: they assess the importance of the nodes merely on the basis on how much they contribute individually to the functioning of the network. As an example, they do not take into account how the network behaves if any subset of nodes (not only a single node) is removed. Moreover, they do not capture some important transportation-related properties. Consequently, existing centrality measures need to be refined, in such a way to take into account that the nodes of the transportation network do not behave merely as individual entities, but as members of coalitions of nodes. The theory of *mathematical games* (Tijs, 2003; González-Díaz et al., 2010), and more specifically, its subfield known as *cooperative game theory*, can be used to deal with the above-discussed drawback. A game describes a situation that involves a set of rational decision makers, called *players*, which are able to make decisions in such a way that each player tries to maximize the payoff obtained as a consequence of the decisions of the whole set of players.

Transportation Network cooperative games (*TNc games*) were defined in Hadas et al. (2017) and further studied in Gnecco et al. (2019). They integrate within a game the topology of the transportation network, the weights of its arcs, and the users' demand, which is modeled by an origin-destination matrix (which contains weights associated with pairs of nodes). Hadas et al. (2017) developed a methodology to assess the importance of the network nodes, taking into account their joint contribution to the overall functioning of the network. Such importance is expressed in terms of a well-known concept from cooperative game theory, namely, the *Shapley value* (Tijs, 2003; González-Díaz et al., 2010). This concept has been recently used in Roson and Hubert (2015) to obtain a measure of the players' power in a network market, and by Li et al. (2018) as a way to assign fair pricing revenue based on each individual contribution. For other applications of cooperative game theory to networks, see, e.g., Lin and Hsieh (2012), van den Nouweland and Slikker (2001), and the references therein. In Gnecco et al. (2021), TNc games were exploited to develop a novel game-theoretic methodology to assess the importance of transfer stops in PT networks. Advantages of the proposed game-theoretic formulation versus classical centrality measures are discussed in depth in Section 2.3 in the above-mentioned work. In the framework considered in that work, transfer times are deterministic. In more realistic situations, however, there can be missed transfers and associated delays. This is the topic of the present work.

1.3. Contributions of this work

Our contributions can be summarized as follows:

- we introduce a stochastic variation of the concept of TNc game, which takes into account stochastic features of PT networks. In this way, a larger variety of network scenarios (possibly with different random network topologies) can be considered with respect to the case of deterministic TNc games. We represent the uncertainty in transfer times via a probabilistic model, which takes into account an additional waiting time whenever a transfer is missed. Transfers are defined as arcs connecting two stops, from which it is possible to change routes. Hence, the

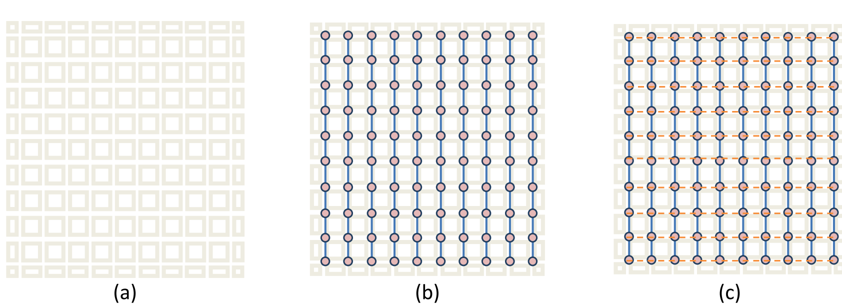

Fig. 1. The "network effect" illustrated with a grid network, adapted from Mees (2010) and Nielsen et al. (2005).

proposed stochastic TNc game integrates properties such as topological connectivity and temporal reliability, providing a means to quantify each transfer's reliability effect on the network performance. This is also in line with Jenelius and Mattsson (2015), as the suggested stochastic TNc game ranks the importance of transfer stops based on their reliability measure, and can assist with the identification of critical ones. The importance of transfer stops in PT networks is then estimated via their Shapley values. Additionally, and following the conclusions regarding the advantages of the proposed modeling over classical centrality measures (Gnecco et al., 2021), the comparison of such measures with the Shapley values is performed;

- we propose an efficient Monte Carlo approximation of the vector of Shapley values (one Shapley value for each player), which takes into account two levels of random sampling (i.e., both permutations of the set of players and stochastic travel times are sampled). This is motivated by the fact that, for a given TU game, an exact computation of the vector of Shapley values typically requires an effort that increases nearly exponentially with respect to the cardinality of the set of nodes (Narayanam and Narahari, 2011). Moreover, in the case of a stochastic TNc game, the realizations of all its random variables should be considered to evaluate exactly the vector of Shapley values, making such evaluation even more computationally demanding than for the deterministic case. Our Monte Carlo approximation is introduced in order to cope with this drawback;

- we make a theoretical analysis of both the proposed stochastic TNc game and of its approximate Monte Carlo solution, investigating its performance;
- we introduce a distributed computing variation of the algorithm by exploiting its special characteristics, so as to reduce its single outer iteration execution time from over 5 min–0.15 min;
- we verify the effectiveness of the proposed method first on a toy-example, then on a real-world PT network from Auckland, New Zealand.

The paper is organized as follows. In Section 2 we model PT networks with stochastic travel and waiting times, then we define TU games tailored to them (s-TNc games), and finally we investigate properties of such games. Section 3 describes and analyzes an algorithm for the approximate evaluation of the vector of Shapley values in s-TNc games. Section 4 illustrates the proposed methodology on a simple toy-network. Section 5 details the case study of a PT network from Auckland, New Zealand. In Section 6, some conclusions are drawn. To make the paper self-contained, main concepts on cooperative games and TNc games are reported in Appendix A and B, respectively. Appendix C is a table with full results for all scenarios and transfers for the network in Section 5. Appendix D contains the proofs of the theoretical results.

2. Stochastic transportation network cooperative games (s-TNc games)

The goal of this section is to propose a stochastic TNc game able to capture the special features of a public transportation network, and to assess the importance of transfer stops taking into account their contribution to the connectivity of the whole network.

2.1. Modelling PT networks with stochastic features

A trip from origin to destination can be abstracted by a sequence of nodes and arcs, representing stops and trip components, respectively. The arcs correspond either to a ride onboard a PT vehicle, or a transfer from one route to another. Considering time as the associated cost, a ride arc cost is the travel time, while a transfer cost is the sum of walking time from one stop to the other (if walking is required) and the waiting time. Each node is not associated with a physical stop, but rather with a logical stop which corresponds to a specific route. Moreover, it is taken into account whether it serves for boarding or alighting. This distinction is required for the evaluation of transfers. Thus, three types of stops are defined: a) origin and destination stops, b) alighting stops, and c) boarding stops. Given the objective, to analyze transfer stops, and the above-mentioned classification, our focus is on the alighting stops, which are the initiators of the transfers.

Fig. 2 (a) illustrates the aforementioned model, with Gi as the origins and destinations stops, T1a, T1b, T1c, T1d, T1e, T1f, T2a, T2b as the transfer stops. The solid nodes are the alighting stops, while the hollow ones are the boarding stops. The solid and dotted lines are the ride and transfer components, respectively. The r_i, are the travel times, whereas the w_{1ij} and the w_{2ij} as the transfer times. Following the definition of alighting and boarding stops, a transfer arc will always start at an alighting stop and terminate at a boarding stop. For example, a trip from G1 to G3 has the following components: 1) a ride onboard a bus from stop G1to stop T1a, 2) a walk to stop T1b, 3) a ride onboard a different bus to stop T2a, 4) a walk to stop T2b, and 5) a ride to G3.

Moreover, for clarity, the network can be presented as an undirected graph, further simplifying the representation, as illustrated in Fig. 2 (b). Each box then represents the logical transfer between a group of routes, and each solid dot models a transfer from the adjacent arc (route) to the other routes. Moreover, each transfer is named after the inbound (alighting stop), i.e., T1f for (T1f, T1b), (T1f, T1d), and (T1f, T1e). One has to bear in mind that this simplification assumes that all stops are bi-directionally connected, hence it should be used only as an overlook at the PT network.

The stochasticity can be referred to the ride and transfer components, as both have random properties. In this paper, it is related only to the costs of the transfer arcs, but it will turn out in Section 2.2 that the formulation can be easily extended to reflect stochastic travel times. Congestion, traffic light delays, demand variations, etc. contribute to that and can be easily estimated based on data collection systems like Automatic Vehicle Location (AVL) systems, which track the movement of PT vehicles, and Automatic Fare Collection (AFC) systems, which record passengers boarding and alighting (Wilson et al., 2009). For each route segment between consecutive stops (r_i), historical travel and dwell times (based on AVL) and historical passengers flows at the stops (based on AFC) can be used to fit a probability density function (pdf). Similarly, the actual transfer times, based on the arrivals and departures times obtained from the AVL data, can be used to fit the transfer time pdf. The transfer time pdf then encapsulates the effect of missed transfers, and as a consequence it reflects the transfers' reliability. Instead of fitting a transfer time pdf, a simpler approach can be used, in which the additional waiting time due to a missed transfer is being represented by a Bernoulli distribution.

Fig. 3 illustrates a toy-example of PT network, having 3 Origin-Destination stops (ODs) - numbered as 1, 2, 3 in the figure -, and 9 transfer stops (the solid dots). Following Fig. 2 (b), each solid dot represents here the alighting stop. The randomness is only associated with the transfer times, as they are the focus of the analysis. Nonetheless, the randomness of travel times could be included as well. Each arc represents a route section connecting two stops. The arcs' values are the travel times. Each solid dot is associated with a Bernoulli distribution and the respected transfer times. For simplicity, all neighbor transfers share the same pdf. In this way, the inner behavior of each box is summarized by that pdf. For instance, in Fig. 3, the transfer time along T1 (the union of T1a and T1b) is 1 unit of time with probability equal to 0.8 (this models the case in which the transfer is not missed), and 1.5 units of time with probability equal to 0.2 (this models the case in which the transfer is missed, hence an auxiliary waiting time is incurred). Finally, still for simplicity, it is assumed here that the ride time is the same for both inbound and outbound directions. In this way, an undirected model is sufficient for the description of the network behavior.

As the goal of our game-theoretic model is to quantify the importance of the transfer stops for what concerns the network connectivity between the ODs, we assume that the latter nodes belong to any

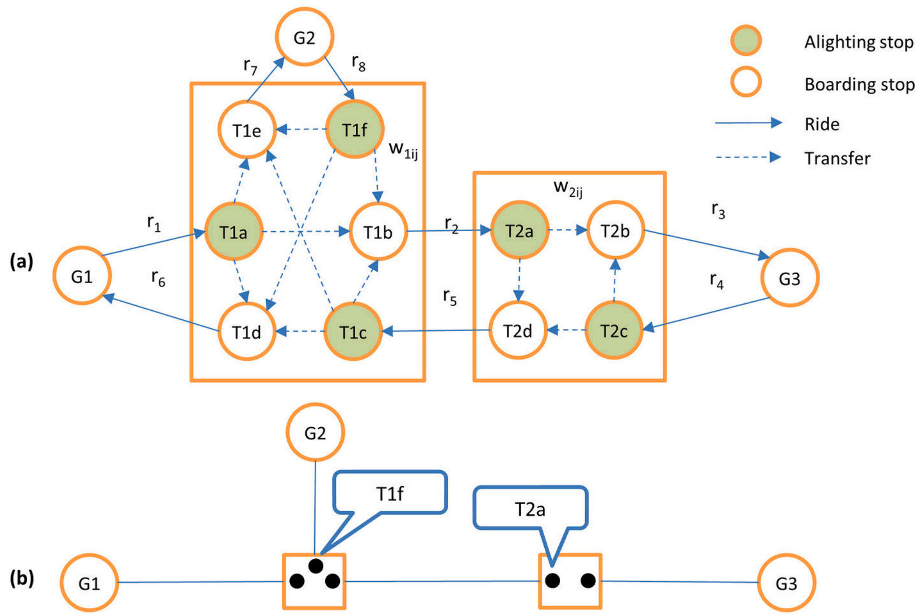

Fig. 2. PT trip abstraction.

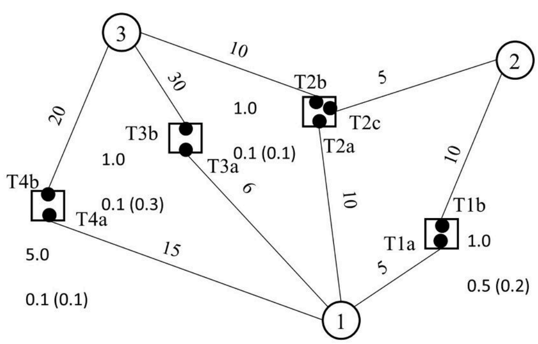

Fig. 3. A simple PT network with stochastic transfer times.

coalition. Hence, in the proposed TNc game, the players are effectively restricted to the transfer stops. In other words, the assessment is based on the impact of the inclusion (or exclusion) of a transfer stop to the connectivity of the whole network.

2.2. Representation of a PT network

Let a stochastic PT network be represented as a graph $G = (V, E, D, W, P^1, P^2)$ with $V = V^g \cup V^a \cup V^b$. Here, V^g is the set of ODs, V^a the set of all alighting stops, and V^b the set of all boarding stops, which are related to trips connecting ODs in V^g. Moreover, let E denote the set of arcs which represent route segments which connect ODs via transfers, so $E_{i\in V^a, j\in V^b}$ is a transfer arc, while all the other elements of E are ride arcs. As V^g is given as an input, E and $V^t = V^a \cup V^b$ are constructed based on the trip legs and transfers required by trips between OD pairs obtained by a PT trip planner such as Open Trip Planner (OpenTripPlanner, 2020), or Google Transit (Google Transit, 2010). Additionally, W is used to define the deterministic time associated with a ride or transfer arc. Finally, D is the demand matrix, i.e., it represents the number of passengers traveling between any OD pair. In other words, in this article the demand is considered as a weight, as detailed later in equation (2). Moreover, D satisfies $D_{i\notin V^g, j\notin V^g} = 0$, meaning that transfer stops can provide a non-zero contribution to the coalition utility only if they connect an OD pair, or improve an existing connection between OD pairs.

To model randomness of the transfer times, two additional matrices are introduced, namely P^1, P^2. P^1 holds the fitted distribution for each arc cost (such as normal, exponential, etc.), and P^2 holds tuples defining the associated parameters (such as (5,2) for a normal distribution or (5) for an exponential one). The matrix $\widetilde{W}$ then can be introduced, which reports the random time associated with each arc:

$$\widetilde{W}_{i,j} = \begin{cases} W_{i,j} + P^1_{i,j}\left(P^2_{i,j}\right) & \text{if } \ i \in V^b \text{and } \ j \in V^a \\ W_{i,j} & \text{otherwise} \end{cases} \tag{1}$$

Note that only the costs of the transfer arcs are modeled as (independent) random variables. Extending the formulation to reflect stochastic travel times is possible with the conversion of the $W_{i,j}$ to probability density functions (pdfs). Moreover, the problem formulation (and the algorithm proposed later in Section 3.1) can be extended with no significant changes to the case of dependent random variables. For the case of both travel time and transfer time randomness, equation (1) can be substituted with $\widetilde{W}_{i,j} = W_{i,j} + P^1_{i,j}(P^2_{i,j})$.

2.3. Mathematical games tailored to stochastic PT networks (s-TNc games)

In this section we introduce a mathematical game able to capture the stochastic features of transfers, as shown in Fig. 3. To this end, we extend to the stochastic framework the (deterministic) TNc games defined in Appendix B. For the readers' convenience, some definitions and concepts on cooperative games are summarized in Appendix A.

In the proposed model, we restrict the players to the transfer stops, and we model the utility $v(S)$ of each coalition (subset) S of players as the difference between the expectations of two suitable random utilities. More precisely, to every coalition $S \subseteq N = V^t$ (including the case $S = \varnothing$), we associate the set $S' := S \cup V^g$, and we denote by $sp(S')$ the matrix containing the lengths of the shortest paths between any two nodes in the subgraph induced by S'. Moreover, we define M as the largest (cost) diameter of any realization of a subgraph of the transportation network, plus 1. Finally, we define the random utility $v'(S') := \sum_{i,j\in S', i\neq j:\ sp(S')_{i,j}<\infty} D_{i,j}(M - sp(S')_{i,j})$, and the (expected) utility

$$\begin{aligned} v(S) &:= E\{v^{'}(S^{'})\} - E\{v^{'}(\varnothing^{'})\} \\ &:= E\left\{ \sum_{i,j\in S^{'},i\neq j:\ sp(S^{'})_{i,j}<\infty} D_{i,j}\left(M - sp(S^{'})_{i,j}\right) \right\} - E\left\{ \sum_{i,j\in \varnothing^{'},i\neq j:\ sp(\varnothing^{'})_{i,j}<\infty} D_{i,j}\left(M - sp(\varnothing^{'})_{i,j}\right) \right\} \end{aligned} \tag{2}$$

where $E\{\cdot\}$ denotes the expectation. Such a utility will be exploited to evaluate the relative importance of each transfer stop. It is worth observing that the constant M is calculated by assuming an unsuccessful transfer on all the stochastic arcs, i.e., by doing a worst-case analysis of the transportation network. The motivation for the presence of the term $E\{v^{'}(\varnothing^{'})\}$ in equation (2) is that, being the players restricted to the transfer stops, such a term may be nonzero. Indeed, some traffic generators may be connected even in the absence of transfer stops. Then, $E\{v^{'}(\varnothing^{'})\}$ is subtracted from every $E\{v^{'}(S^{'})\}$, defining a utility function $v(S)$ for which the assumption $v(\varnothing) = 0$ is automatically satisfied. In doing so, no change occurs in the (expected) marginal utility values. We call the above-defined TU game *stochastic TNc game* (or *s-TNc game*, for short).

For each player i, its Shapley value takes the following form:

$$\begin{aligned} Sh(i) :&= \sum_{S\subseteq N}\left((v(S) - v(S\backslash\{i\}))\frac{(|S|-1)!(n-|S|)!}{n!} \right) \\ &= \sum_{S\subseteq N}\left((E\{v^{'}(S^{'})\} - E\{v^{'}(S^{'}\backslash\{i\})\})\frac{(|S|-1)!(n-|S|)!}{n!} \right) \end{aligned} \tag{3}$$

In the particular case in which, for each coalition S, the set of the shortest paths (see Appendix B) does not depend on the randomness of the arcs, in order to compute the Shapley values one can effectively replace the graph (V, E, D, W, P^1, P^2) with a deterministic one, having the weight matrix with elements $E\{\widetilde{W}_{i,j}\}$. Indeed, in this particular case, the equation (3) reduces to the definition of Shapley value in the deterministic case.

The main property of the model refers to the case of an undirected graph (V, E, D, W, P^1, P^2), and allows to express the expected utility $E\{v^{'}(S^{'})\}$ associated (via $S^{'}$) to any subset S of transfer stops (which is used to express $v(S)$ in equation (2)) in terms of the connected components of its (random) induced subgraph.

Proposition 1. Let the graph (V, E, D, W, P^1, P^2) be undirected, and, for each realization of it, let the subgraph induced by a subset $S^{'}$ of nodes be made of $C_{S^{'}}$ connected components whose sets of nodes are indicated as $S'_1, \ldots, S'_k$, respectively. Then

$$E\{v^{'}(S^{'})\} = E\left\{ \sum_{k=1}^{C_{S^{'}}} \sum_{i,j\in S'_k, i\neq j} D_{i,j}\left(M - sp(S'_k)_{i,j}\right) \right\} \tag{4}$$

Proposition 1. *can be extended to the case of directed graphs, simply by replacing connected components with weakly connected components, i.e., maximal directed subgraphs for which, for each pair of vertices i,j in the subgraph, there are both a directed path from i to j and a directed path from j to i.*

It is worth noting that, when the randomness of the arcs does not modify the connectivity properties of the network (*i.e., when the set of indices of finite entries in the matrix* $\widetilde{W}$ *in* Section 2.1 *does not depend on the realization of the matrix*), *the connected components of any induced subgraph of* (V, E, D, W, P^1, P^2) *do not depend on the realizations of the stochastic arcs. In this case, the number* $C_{S^{'}}$ *of connected components and the sets* S'_k *in the* equation (4) *becomes deterministic, so it can be replaced by*

$$E\{v^{'}(S^{'})\} = \sum_{k=1}^{C_{S^{'}}} \sum_{i,j\in S'_k, i\neq j} D_{i,j}\left(M - E\left\{sp(S'_k)_{i,j}\right\}\right) \tag{5}$$

In the general case, however, the connected components and their number depend on the realizations of the stochastic arcs, hence they are random. This holds also for the identities of the arcs that constitute shortest paths in $sp(S'_k)$.

Proposition 2. *The utility function* $v(S)$ *in* equation (2) *is monotonic, i.e., for every two sets S and T with* $S \subseteq T \subseteq N$*, one has* $v(T) \geq v(S)$.

3. Calculation of the Shapley value for s-TNc games

3.1. The Stochastic TNc-ApproShapley algorithm

For deterministic TNc games, an approximation $Sh^{'}$ of the vector Sh of Shapley values can be computed using the Monte Carlo approximation algorithm (called ApproShapley) presented in Castro et al. (2009). It is based on the fact that the Shapley value of a player i represents the average marginal utility of that player when it enters a random coalition (Tijs, 2003; González-Díaz et al., 2010). In Hadas et al. (2018), the ApproShapley algorithm was found to be quite accurate through simulation results, taking the classical Sioux Falls network as a test-bed. Moreover, a revised and even more efficient version of the algorithm (named TNc-ApproShapley) was developed therein, taking into account the specific form of the utility function in a TNc game. In more details, in Hadas et al. (2018), Floyd-Warshall's algorithm was used for the determination of the sets of the shortest paths, as it allows some simplifications in the computation of the utility value for different coalitions. These are due to its internal use of dynamic programming, which avoids duplicating some computations. It is worth noting that, for deterministic TNc games, the ApproShapley and the TNc-ApproShapley algorithm produce exactly the same output: the difference is only in the required computational time.

Here a stochastic extension of the TNc-ApproShapley algorithm is proposed (Algorithm 1). It takes into account the reliability properties of the arcs, by generating random realizations of the graph according to equation (2).

Given a game having a set N of players, let m be a permutation of the set of all its players, in which the player $m(k)$ appears in the position k. Moreover, let $M(N)$ denote the set containing all the permutations of the set N. For a given permutation m, let $Pre_m(i)$ denote the set of the predecessors of the player i in such a permutation, i.e., $(m(i), \ldots, m(i-1))$ or the empty sequence in the case in which $i = 1$. Finally, fix a number S_P for the number of permutations considered, and a number N_R of random realizations of the graph.

$C_{INNER} = 0, C_{OUTER} = 0, sh^{'} = 0$

While $C_{OUTER} < S_p(outer\ \ level)$

Take $m \in M(N)$ with probability 1/n!

While $C_{INNER} < S_p(outer\ \ level)$

Generate independent realizations $\widetilde{W}_{i,j}$ based on $P^1_{i,j}$ and $P^2_{i,j}$:

$$\widetilde{W}_{i,j} = \begin{cases} W_{i,j} & \forall i \notin V^b, j \notin V^a \\ W_{i,j} + P^1_{i,j}\left(P^2_{i,j}\right) & \forall i \in V^a, j \in V^b \end{cases}$$

$vp := v'(V^g)$

For all $i = m(1), ..., m(N)$

Compute $vc := v'(Pre_m(i) \cup \{i\} \cup V^g)$ using Floyd-Warshall's algorithm

Compute $x_p(i) := vc - vp$

$Sh'(i) := Sh'(i) + x_p(i)$

$vp := vc$

End

$C_{INNER} := C_{INNER} + 1$

End

$C_{OUTER} := C_{OUTER} + 1$

End

$Sh'(i) := Sh'(i) / (S_P N_R) \forall i \in N$

Algorithm 1. - The stochastic TNc-ApproShapley algorithm

3.2. Properties of the proposed stochastic TNc-ApproShapley algorithm

The proposed stochastic TNc-ApproShapley algorithm outputs, for every player i, an approximation $Sh'(i)$ of its Shapley value $Sh(i)$ in the stochastic TNc game. Such algorithm differs from the ApproShapley algorithm considered by Castro et al. (2009), as it belongs to the family of 2-level Monte Carlo algorithms (Ryan, 2003). These are characterized by the presence of both a first (outer) loop of random sampling, and a second (inner) loop of random sampling. In our algorithm, a random permutation is generated in the outer loop (for a total number of S_P such permutations). In the inner loop, instead, one generates, independently from the previous permutation, a set of random values for the costs of the arcs in the graph (for a total number of N_R such sets).

The stochastic TNc-ApproShapley algorithm can be investigated following the lines of the analysis of the 2-level Monte Carlo algorithm reported in Section 3 of Ryan (2003), which was used in that work for a different problem in Bayesian optimal design.

Unbiasedness of the estimate $Sh'(i)$

Differently from the case of the problem investigated in Ryan (2003), the estimate $Sh'(i)$ computed by the proposed stochastic TNc-ApproShapley algorithm is unbiased, as stated in the next proposition.

Proposition 3. *The estimate $Sh'(i)$ is unbiased, i.e., $E\{Sh'(i)\} = Sh(i)$.*

Upper bound on the variance of the estimate $Sh'(i)$

The next proposition bounds from above the variance

$$\mathrm{var}\{Sh'(i)\} := E\left\{(Sh'(i) - E\{Sh'(i)\})^2\right\} = E\left\{(Sh'(i) - Sh(i))^2\right\} \tag{6}$$

of the approximation $Sh'(i)$ obtained by the stochastic TNc-ApproShapley algorithm.

Proposition 4. *Let S_P be the number of permutations of the players considered and N_R the number of realizations of the graph considered. The following upper bounds hold for the variance $\mathrm{var}\{Sh'(i)\}$:*

$$\text{(i)}\quad \mathrm{var}\{Sh'(i)\} \leq \frac{A}{S_P} + \frac{B}{S_P N_R} \tag{7}$$

where $A \geq 0$ and $B \geq 0$ depend on the instance of the stochastic TNc game;

$$\text{(ii)}\ \mathrm{var}\{Sh'(i)\} \leq \frac{v'_{\max}(N)}{2} \cdot \frac{N_R + 1}{S_P N_R} \tag{8}$$

where $v'_{\max}(N)$ is the maximum realization of the random utility $v'(N)$ of the grand coalition.

For a given upper bound on $\mathrm{var}\{Sh'(i)\}$, the bound from Proposition 4 (ii) can be used to choose the parameters S_P and N_R in such a way to satisfy the bound. In practice, the bound shows that, for N_R sufficiently large, only the choice of S_P is important to further reduce the upper bound on the variance of the proposed approximation $Sh'(i)$ of each Shapley value $Sh(i)$. However, it is worth noting that the resulting guarantees on such estimates are merely probabilistic. Moreover they may be loose, since the bound from Proposition 4 (ii) may not be tight. In practice, an empirical estimate of $\mathrm{var}\{Sh'(i)\}$ can be exploited instead of that bound, simply by computing the empirical variance of several independent realizations of $Sh'(i)$.

The drawback of calculating the empirical variance (or empirical standard deviation) is when the computation time of S_P permutations is long (assuming a fixed value of N_R has been exploited). In such a case a different approach can be used, which is based on the Shapley values convergence $Sh''_r(i) := \frac{Sh''_{r-1}(i) \cdot S_P \cdot (r-1) + Sh'_r(i) \cdot S_P}{S_P \cdot r}$, where $Sh''_r(i)$ is the cumulative Shapley value for permutations from 1 to r, averaged for each permutation over the N_R realizations of the stochastics weights.

Then the deviation (or error) can be calculated as

$$\Delta Sh_r(i) = \frac{Sh''_r(i) - Sh''_{r-1}(i)}{Sh''_{r-1}(i)} \tag{9}$$

as well as the average and maximal error, respectively:

$$\overline{\Delta Sh_r} = \sum_{i=1}^{|N|} \frac{\Delta Sh_r(i)}{|N|} \tag{10}$$

$$\overline{\overline{\Delta Sh_r}} = \max_i (\Delta Sh_r(i)) \tag{11}$$

Given a predefined error threshold, the Stochastic TNc-ApproShapley algorithm will be executed repeatedly with S_P permutations, until either the calculated error $\overline{\Delta Sh_r}$ or $\overline{\overline{\Delta Sh_r}}$ reaches the threshold.

3.3. Efficient distributed computing implementation of the algorithm

As the outer iterations are independent of each other, and the Shapley value approximation is the average of all the outer iterations, a distributed computing implementation of the Stochastic TNc-ApproShapley algorithm is possible.

Thus, the total number S_P of outer iterations can be nearly evenly split between identical CPU cores, so each CPU core (or worker) can execute its portion of code in parallel to the other CPU cores.

The distributed version of the Stochastic TNc-ApproShapley algorithm then can be constructed as follows.

1. Let N_{CPU} be the number of available CPU cores, denote the core of each CPU as $c = 1, ..., N_{CPU}$, and let $S_{P,PAR} = \left\lceil \frac{S_P}{N_{CPU}} \right\rceil$ as the number of outer iterations per CPU core.
2. Execute N_{CPU} instances of the Stochastic TNc-ApproShapley algorithm in parallel, substituting S_P with $S_{P,PAR}$ and $Sh'(i)$ with $Sh'(i,c)$.

3. Compute the aggregated Shapley value approximation as $Sh^{'}(i) = \frac{\sum_{c\in\{1,\ldots,N_{CPU}\}} Sh^{'}(i,c)}{N_{CPU}}$.

For the speed-up evaluation related to the number of CPU cores, Ray (Moritz et al., 2018) – which is a distributed framework that can combine several computers (or virtual machines) into a single cluster – was used. Ray is a distributed execution framework that aims to provide a universal API for distributed computing. The framework allows executing a program script from one main machine (head) and executing it across several machines simultaneously (workers) while Ray manages the scheduling and autoscaling of the resources across the machines.

As Ray has a theoretically unbounded maximum number of workers, the only limitation for analyzing large-scale networks will be the number of machines available to be used as workers. For this work, 4 Ubuntu 20.04 LTS servers running on Microsoft Azure cloud services were used. Each machine has the same configuration of 72 CPU cores and 144 GB of RAM. Combining Ray's abilities alongside such powerful machines allows us to execute the algorithm using a total of 288 CPU cores. Fig. 4 illustrates the advantages of distributed computing versus non-distributed implementation, with execution speed-up from ~5 min with a single CPU core (non-distributed implementation) to ~0.15 min with 144 CPU cores.

4. Illustration of the methodology on a simple network

The Stochastic TNc-ApproShapley algorithm was used to evaluate four scenarios for the PT network presented in Fig. 3. S_P was set with increments of 1000 (1000, 2000, etc.), until the average error was less than 2% (~50 increments, or $S_P = 50000$). N_R was set equal to 10. Furthermore, for the first scenario, which is deterministic, the TNc-ApproShapley algorithm was used for the validation. For simplicity, we assumed the same demand for all the ODs. The first case, i.e., the deterministic one, acts as a term of comparison for the other stochastic scenarios. In this scenario, every transfer is successful, and $\widetilde{W}_{i,j} = W_{i,j}$ for all i and j. Scenarios 2 and 3 model isolated cases when T4 or T2 transfers have a 0.1 probability for missed transfers with an additional waiting time of 10 time units, respectively. Scenario 4 reflects the case when finite delays may occur when transferring. It is provided in order to illustrate the situation in which all transfer times are stochastic.

4.1. Centrality measures comparison (deterministic scenario)

First, a comparison with two common centrality measures was carried, similar to Gnecco et al. (2021). Both the weighted closeness and weighted betweenness were compared based on the deterministic scenario. Table 1 summarizes the results of the analysis obtained for each transfer. The actual results are for reference, as only the normalized results (expressed, for each centrality measure, as percentages with respect to the sum of its outcomes over the transfers) are comparable.

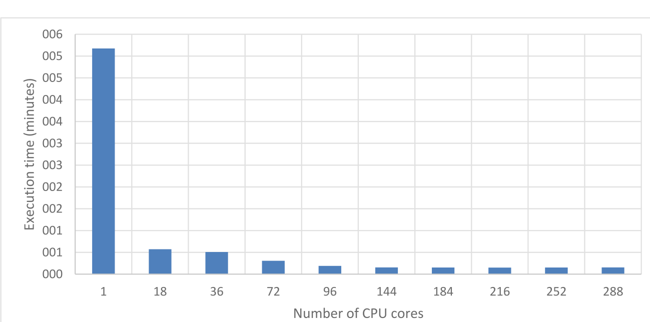

Fig. 4. Execution speed-up time related to the number of CPU cores.

The results confirm that the closeness measure poorly performs by providing a uniform-like distribution of the importance (9%–14%) with the most important transfer (T2b) having not so different importance from T1a, T1b, T2b, and T2c (14% versus 12%). The betweenness measure performs much better and captures the most important transfer (T2a). However, as this measure counts the number of shortest paths a node residing at, it does not consider other alternative routes. Specifically, there are two identical routes connecting nodes 1 and 2, where one involves T2a and the other involves T1a, hence T2a importance is lower when considering the Shapley value. Similarly, T2b is ranked number 2 when betweenness is calculated. However, nodes 1 and 3 have 2 other (although longer) alternatives. This is why transfer T2b is not ranked 2nd. Additionally, transfers T3a, T3b, T4a, and T4b have higher Shapley values.

Moreover, the classical centrality measures do not take into account demand (or node weights), which is a critical component in the context of transport network analysis. The reader is referred to Section 2.3 of Gnecco et al. (2021) for a further discussion on this issue.

Finally, when assessing a network with stochastic properties, the classical centrality measures cannot consider the travel time increase caused by transfers reliability. On the other hand, TNc games have a unique property – the Shapley value is the average marginal utility value, hence the summation of all the average marginal utilities is meaningful and represents the total utility of the grand coalition. As the grand coalition is the whole network, and the demand is weighted, the utility value is the actual total travel time saving. Unlike that, for most classical centrality measures, summing up such measures over all the nodes has no immediate meaning. The next section will take advantage of the average marginal utility value summation as a proxy for reliability.

4.2. Reliability analysis

In this section, the reliability analysis of each transfer is assessed based on its individual effect on the total utility value. Loosely speaking, transfers are considered reliable in a specific stochastic scenario if suitable performance indicators (e.g., the total utility or each transfer's importance) do not change significantly when moving from the deterministic to the stochastic scenario. It is worth noting that the ranking of transfers for a given scenario does not provide any insights on reliability, but only on the importance of each transfer with respect to all other transfers. This, by itself is a valuable information, however not different from the analysis reported in Gnecco et al. (2021) for the deterministic case. As the main outcome of reliability analysis is the increase of travel time (due to the additional waiting time caused by stochasticity), reliability can be associated with the change in each Shapley value.

For an evaluation of the reliability, the two following indicators are computed, by comparing every specific scenario to the deterministic (baseline reference) one: 1) ORO (Overall Reliability Outcome), which is the reduction in the total utility, and 2) TRO (Transfer Reliability Outcome), which expresses the change in each transfer's importance. The ORO refers to the performance of the network in terms of travel time delays, i.e., the decrease in travel time saving caused by moving from the deterministic to the stochastic scenario. Such a decrease is a first possible way of expressing reliability. As the deterministic scenario reflects the planned travel times, it serves as the baseline for the utility value. When compared to a stochastic scenario, the change is the effect of the specific scenario's reliability. The TRO identifies those transfers that are mostly impacted by the change, i.e., their Shapley value significantly decreases, compared to the deterministic (baseline) scenario. This is a second possible way of expressing reliability.

Based on the ORO and TRO, the following situations can occur:

1. Small change in ORO: no major impact on the network performance, since unreliable transfers (negative TRO) are being compensated by alternative transfers (positive TRO), which belong to slightly longer

Table 1
Centrality measures comparison for the deterministic scenario.

	Centrality measures			Normalized centrality measures		
Transfer	Closeness	Betweenness	Shapley value	Closeness	Betweenness	Shapley value
T1a	0.0032	51	58.7	11.7%	11.6%	13.0%
T1b	0.0033	51	57.9	11.8%	11.6%	12.8%
T2a	0.0038	132	113.7	13.7%	30.0%	25.2%
T2b	0.0034	83	55.2	12.3%	18.9%	12.2%
T2c	0.0033	47	59.5	12.0%	10.7%	13.2%
T3a	0.0028	19	27.8	10.3%	4.3%	6.2%
T3b	0.0030	19	27.7	10.7%	4.3%	6.1%
T4a	0.0024	19	25.5	8.8%	4.3%	5.6%
T4b	0.0024	19	25.9	8.7%	4.3%	5.7%

Table 2
Results for the four considered scenarios. The notations T4 (10, 0.1) and T2 (10, 0.1) mean that transfer T4 (respectively, T2) incurs an additional waiting time of 10 time units with probability 0.1

Scenario Transfer	1 Deterministic	2 Stochastic T4 (10, 0.1)	3 Stochastic T2 (10, 0.1)	4 Fully stochastic
(Approximate) Shapley values				
T1a	58.7	56.6	113.8	8.6
T1b	57.9	56.0	113.5	9.2
T2a	113.7	126.5	1.4	135.5
T2b	55.2	69.6	0.8	50.5
T2c	59.5	56.8	1.0	84.6
T3a	27.8	42.8	42.0	9.7
T3b	27.7	43.1	41.2	10.1
T4a	25.5	0.3	37.0	22.0
T4b	25.9	0.3	37.6	21.9
Total Utility	452.0	452.0	388.4	352.0
Utility reduction		0.0	63.6	100.0
Normalized (approximate) Shapley values				
T1a	13.0%	12.5%	29.3%	2.4%
T1b	12.8%	12.4%	29.2%	2.6%
T2a	25.2%	28.0%	0.4%	38.5%
T2b	12.2%	15.4%	0.2%	14.3%
T2c	13.2%	12.6%	0.3%	24.0%
T3a	6.2%	9.5%	10.8%	2.8%
T3b	6.1%	9.5%	10.6%	2.9%
T4a	5.6%	0.1%	9.5%	6.3%
T4b	5.7%	0.1%	9.7%	6.2%
Difference with respect to the deterministic case				
T1a		−2.1	55.1	−50.1
T1b		−2.0	55.6	−48.8
T2a		12.8	−112.3	21.7
T2b		14.4	−54.4	−4.7
T2c		−2.7	−58.5	25.1
T3a		14.9	14.2	−18.1
T3b		15.4	13.5	−17.6
T4a		−25.2	11.5	−3.5
T4b		−25.6	11.6	−4.0

routes. The network is resilient to the specific scenario's stochastic properties.

2. Large change in ORO: major impact on the network performance, TRO has to be further analyzed. By identifying transfers with large and negative TRO (i.e., transfers that mostly negatively impact the performance), transportation planners are able to focus their successive analyses on such transfers in order to identify the cause for such an outcome and to implement a possible remedy.

Table 2 gives a summary of the results of the evaluations of all the scenarios considered in our analysis, by reporting the approximate Shapley values, their normalizations (i.e., the approximate values divided by their summation), and the differences between the approximate Shapley values as calculated in every scenario and the ones obtained in Scenario 1 (the deterministic one). The ORO is not affected in Scenario 2, as its stochastic transfer (T4) is not part of the shortest path between nodes 1 and 3. However, in Scenarios 3 and 4 the ORO is reduced, as the transfer along T4 is on the shortest path between nodes 1, 2 and 3. As a consequence any delay on it will increase the total travel time, and as a result, reduce the utility value. Moreover, the most critical transfers have both negative ORO and negative TRO (e.g., T2a, T2b, T2c in scenario 3, T1a, T1b in scenario 4), as the decrease in the transfer's performance (i.e., a decreased approximate Shapley value) highly influences the overall network performance. To conclude, it is worth mentioning that, in Table 2, the total utility (i.e., the utility if the grand coalition) is the same for both the deterministic and the first stochastic case (the one associated with T4). This depends on the fact that, when considering the whole network, the stochastic arcs do not appear in any shortest path. Nevertheless, they are used in some shortest paths belonging to subnetworks corresponding to specific smaller coalitions of transfers. This reduces the utility of such coalitions and, as a consequence, affect the Shapley values (being them the average marginal utilities of the transfers). Finally, it is also worth observing that the Shapley values reported in the various columns of the table (and also the most critical transfers identified in the various cases) are different because they refer to different stochastic perturbations of the original deterministic network.

5. The Auckland case study

A case study for the Auckland bus network was conducted based on the following data sources from 2010: 1) APT3 (Auckland Passenger Transport model) AM peak PT demand forecast at the transportation zone level, 2) the PT network obtained from the general transit feed (GTFS) dated May-3, and 3) AVL data for the whole month of May.

The data preparation process was comprised of three steps: 1) selecting origin and destination stops, 2) constructing the PT network (ride and transfer components), and 3) analyzing transfers stochasticity.

5.1. Origin-destination stops selection

Only a subset of all OD pairs was selected for analysis, in order to focus on routes with sufficient demand. For that, based on the zonal demand forecast matrix, only zones pairs with demand higher than 15 passengers per hour were selected. Moreover, close proximity zones (less than 2 km) were discarded, as walking and cycling might be preferred modes.

All stops within the boundaries of each zone were selected as origin and destination stops. All stops within a buffer of 100 m outside each zone were included as well. The centroid of each zone was connected with zero weight dummy links to all associated stops. A total of 191 origin stops and 56 destination stops were obtained. Fig. 5 presents the selected zones, the zones pairs, and the relevant stops. The zone pairs are connected with variable width gray lines, reflecting the relative demand. Origin stops are marked with green dots and destination stops with orange dots. The transfer nodes are marked with blue dots and will be discussed in the next section.

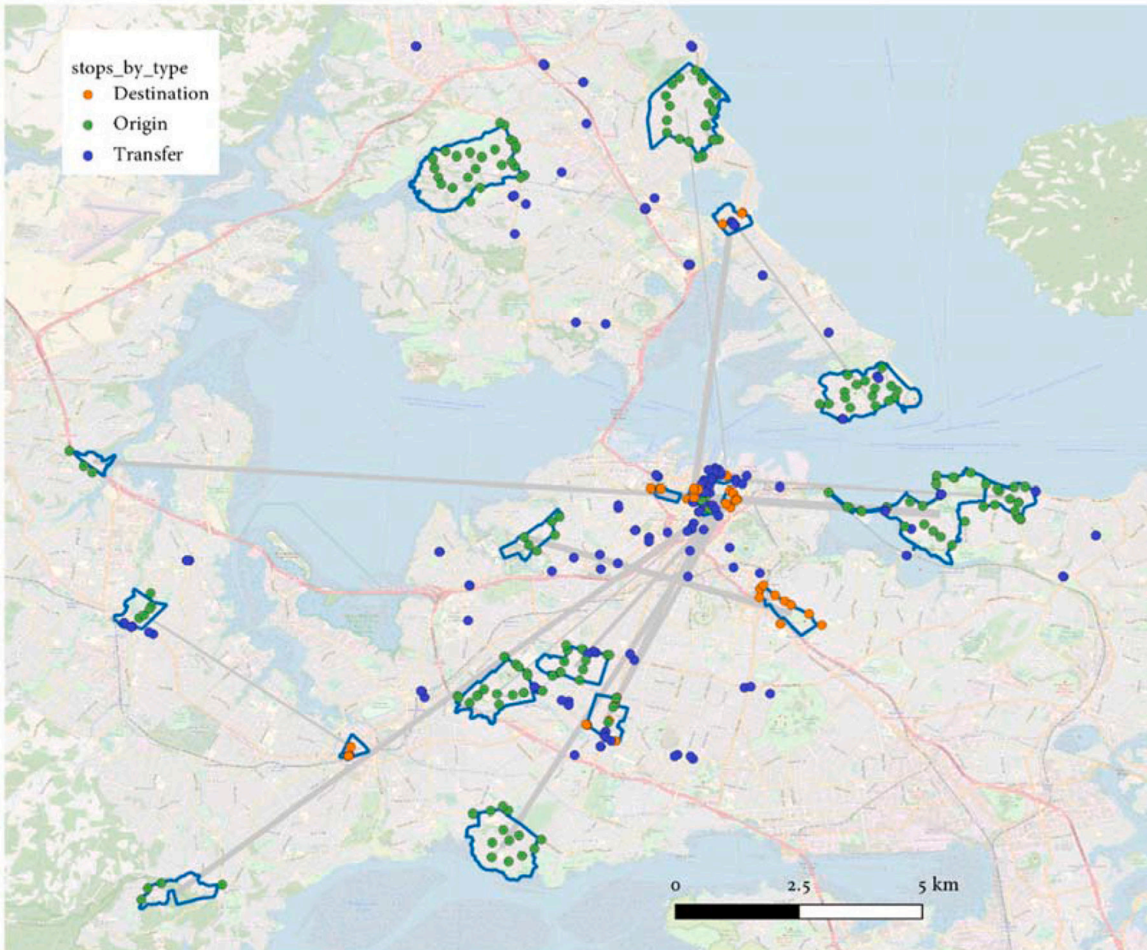

Fig. 5. The Auckland PT network.

5.2. Network construction

Given the set of origin and destination stops, PT itineraries were generated by the Open Trip Planner – OTP (OpenTripPlanner, 2020), an open source trip planner. The OTP requires a GTFS complaint dataset and an OpenStreetMap (OpenStreetMap, 2012) road layer for the analyzed area. The OTP can be used in two modes, interactive and batch. The former is the mode used to plan interactively a trip by the user, while the latter is the recommended mode for extracting a large set of trips. The above-mentioned set of stops was used as the input for the OTP. The date selected was May-3, 7–9AM, with two potential modes, "walk" and "bus". For each OD pair, three itineraries were generated at the most. Table 3 illustrates the results of the extraction process. Each line represents a trip leg, including the start and finish stops, mode, ride/walk times, waiting times, and distance. The itineraries obtained serve two purposes: 1) constructing the PT network, i.e., the route segments connecting stops, along with the planned ride times and transfer times (walk time + waiting time), and 2) the identification of the stops serving as transfers. A total of 152 transfer stops were identified, which are marked with blue dots in Fig. 5. However, these are physical stops, which might serve several routes, in contrast to the model that requires logical stops, each serving only one route. Hence a total of 167 transfers stops were generated.

5.3. Transfer times' distributions analysis

The last step required to fit a distribution to each transfer obtained in the second step. As each transfer is uniquely defined by inbound and outbound routes at their respective alighting and boarding stops (herein referred to as A and B respectively), the associated AVL data can be used to extract historical transfer times. More specifically, all AVL data recorded during the month of May for weekdays and the morning peak were extracted and matched in the following way. For each arrival at A, the closest departure from B, which is largest than the walking time, was selected. Then, for each of these pairs, the transfer time was calculated as the difference between departure from B and arrival at A.

Table 3
Sample output from the OTP extraction tool.

Itinerary	Leg	Mode	Route	Head sign	From stop	To stop	Ride/walk time	Waiting time	Distance
1	0	BUS	769	ST HELIERS	37	7334	4	0	2178
	1	WALK	0				0.1	2	5
	2	BUS	767	BRITOMART	7335	7010	22	0	7320
	3	WALK	0				3	8	233
	4	BUS	LINK	VICTORIA PRK	7016	9106	9	0	1528

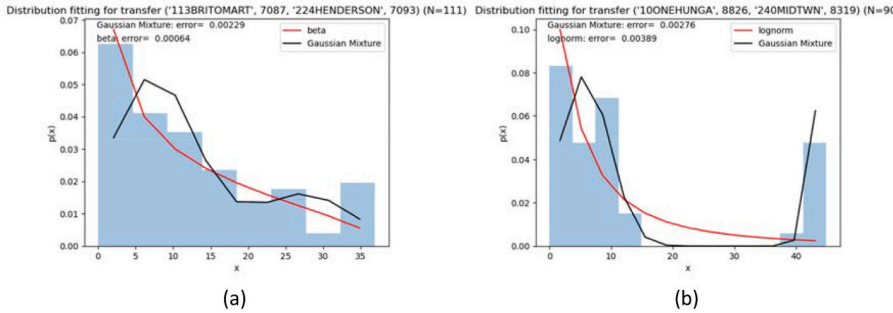

Fig. 6. Unimodal and multimodal distributions and best fitted continuous distributions.

Unimodal and multimodal fitting algorithms were used to find the best matched distribution for each transfer. A unimodal distribution, which has a single peak (mode), best describes situations in which the transfer time variability is mostly associated with the random arrival of a given planned trip (Fig. 6, a). A multimodal distribution (Fig. 6, b), on the other hand, is characterized by several peaks (modes) each related to a different planned trip. In other words, when the headways are large, and missed transfers occur, the historical AVL data represent a mixture model, which is a combination of several distributions, each related to a different planned trip.

For the unimodal distribution, the Python FITTER package (Cokelaer, 2019) was used. For the multimodal one, a Gaussian Mixture algorithm was applied, which is defined as “a probabilistic model that assumes all the data points are generated from a mixture of a finite number of Gaussian distributions with unknown parameters” (Pedregosa et al., 2011). For each transfer both algorithms were executed, with the distributions having the least error being selected. As a result, the following distributions were selected: Beta (18%), Exponential (4%), Gamma (11%), Gaussian Mixture (40%), Lognormal (24%), and Triangular (3%).

5.4. Results and analysis

The Stochastic TNc-ApproShapley Algorithm (as well as the deterministic one) were implemented with Python 3.8, taking advantage of its multiprocessing capabilities. The code was executed on a two Linux Virtual Machines (VM), F-Series v2 CPU, each with 72 cores. S_P was set with increments of 1000 (1000, 2000, etc.), until the average error was less than 2% (~50 increments, or $S_P = 50000$), as illustrated in Fig. 7. The number N_R of random realizations of the graph was set to 10. The deterministic and stochastic algorithms execution times were 5 h and 18 h, respectively.

Three scenarios were examined: ideal, deterministic, and stochastic. The ideal scenario represents a non-existent situation (hence the term ideal), in which all the transfers are instantaneous. This scenario serves as a reference point for the quantification of the contribution of the transfers to the overall utility. The deterministic scenario considers the transfer times as constant, and equal to the planned transfer times obtained from the OTP. The stochastic scenario has stochastic transfer times based on the above-mentioned fitting procedure. All the scenarios consider ride times as constant, based on the OTP.

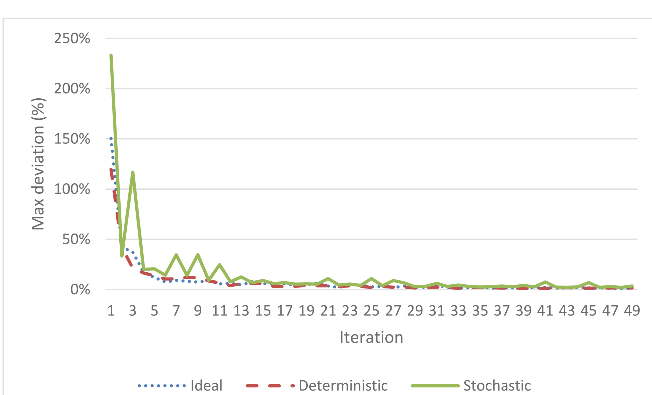

Fig. 7. Algorithm’s deviation convergence.

First, the model was compared to classical centrality measures (closeness and betweenness) in order to demonstrate its advantages. This analysis was based on the deterministic scenario and did not consider demand, as the closeness and betweenness measures are deterministic and cannot integrate a weight matrix. Second, the ORO and TRO measures were used to analyze the network’s transfers reliability.

5.4.1. Comparison with classical centrality measures

Following Section 4.1, the results obtained for the Auckland’s deterministic scenario (with uniform demand) were compared to the closeness and betweenness centrality measures. Table 4 provides a simple comparison of the transfers’ importance (normalized) distributions of the 167 transfers. Each row provides the statistics per bin, or interval, both as absolute values (number of occurrences) and relative values (percentages). For example, 78 transfers have zeros Shapley value, in contrast to 0 and 5 for closeness and betweenness, respectively. Note that normalized closeness centrality values are concentrated in the interval [0.2%, 2%]. The normalized betweenness centrality has a distribution similar to that of the normalized closeness centrality, with higher concentration in the interval [0.2%, 1%). Instead, the TNc measure identifies almost 50% of the transfers as non-relevant (with zero Shapley value), meaning that they do not dominate other transfers. Please recall that the transfers were obtained by enumerating a trip planner result based on three trips for each origin-destination pair, this implies that some trips are non-relevant and are not being used at all (zero utility value). This phenomenon was not captured by the closeness and betweenness measures. Moreover, 7% of the transfers have normalized Shapley value larger than 2, which is in line with the results obtained in Gnecco et al. (2021). Finally, notice that the analysis for the stochastic scenarios reported in the remaining of this section is made only for the Shapley values, because it cannot be performed based on the closeness or the betweenness measures, as stated at the end of Section 4.1.

Moreover, drilling-down and analyzing the top-5 transfers for each centrality measure, reveals that there is hardly any correlation between any two such measures (Table 5) and that the TNc measure better captures the transfers’ importance when considering the actual location of the transfers (Fig. 8). Based on the authors’ knowledge of the Auckland’s PT network, it was possible to investigate actual transfers (numbered labels on Fig. 8), and comment on their importance. Both closeness centrality and betweenness centrality wrongly identify transfers on a) the northern motorway (663, 687, 688) which does not provide major transfer at the network level, and b) transfers not on the direct routes to

Table 4
Auckland PT network centrality measures comparison.

Normalized value (%)	Number of occurrences			Percentage		
	Shapley value	Closeness	Betweenness	Shapley value	Closeness	Betweenness
=0	78	0	5	47%	0%	3%
∈ (0, 0.2]	21	19	75	13%	11%	45%
∈ [0.2, 1)	22	119	57	13%	71%	34%
∈ (1, 2]	34	28	21	20%	17%	13%
∈ (2, 3]	9	1	3	5%	1%	2%
∈ (3, 4]	2	0	2	1%	0%	1%
∈ (4, 6]	0	0	2	0%	0%	1%
>6	1	0	2	1%	0%	1%

Table 5
The top 5 important transfers by centrality measure.

Order by	Transfer ID	Shapley value	Closeness	Betweenness
Shapley value	692	8.18	0.33	0.74
	760	3.53	1.93	2.18
	754	3.26	0.62	0.24
	776	2.97	0.73	1.12
	818	2.84	0.87	0.66
Closeness	757	1.72	2.01	1.88
	760	3.53	1.93	2.18
	718	0.03	1.85	7.74
	687	0.00	1.76	8.56
	688	0.00	1.57	1.78
Betweenness	687	0.00	1.76	8.56
	718	0.03	1.85	7.74
	741	0.00	1.09	4.31
	663	0.00	1.53	4.28
	817	0.31	1.33	3.88

and from the city center (718, 817). On the other hand, these measures do not identify Newmarket hub (692), or transfer at arterial roads (776, 818). This suggest that the real-world usefulness of the classical measures is questionable, in addition to their inability to capture demand and stochasticity.

5.4.2. *Transfers reliability analysis*

As mentioned, three scenarios were examined reflecting the characteristics of transfers waiting times: ideal, deterministic, and stochastic.

The analysis is summarized in Table 6, which provides a comparison between the scenarios for 7 bins (or intervals) based on the normalized Shapley value (zero, in (0%, 1%], in (1%, 2%], etc.). For each interval, the number of transfers and the sum of the Shapley values are reported (absolute and relative). For all scenarios, a small set of transfers (~10%) contributes to ~50% of the total utility (marked bold), implying their high contribution to the connectivity of the whole network. Moreover, the direct (caused by waiting) and indirect (caused by using an alternate route) effect of the transfers reliability (for the stochastic scenario) has a penalty of 177,569 min, compared to the deterministic scenario (49,400) which is over 3 times larger than the penalty occurred by the planned transfer times. Another interesting observation is that ~50% of the transfers obtained by the trip planner do not contribute to better connectivity (normalized Shapley value of 0), which is aligned with the results obtained in Section 5.4.1. The main reason is that these transfers are part of a multi-legged trips, which once constructed are inferior to previously selected trips.

Fig. 9 shows the stochastic scenario's normalized Shapley values per stop, where stops with a cross have zero Shapley value, while the light-colored dots have lower values as opposed to the dark-colored dots. The important transfers are located at the city's center and at Newmarket (the dark dot at the lower left). When considering the TRO (Transfer Reliability Outcome) due to the stochasticity of the transfers' times (Fig. 10), it is evident that most transfers have a small negative TRO, meaning that their impact on the networks' reliability is small (light yellow), and only a small number of stops have a large negative TRO (marked red), meaning that they have the highest impact on the network's reliability. On the other hand, blue dots represent those transfers that have increased importance, as they are being used as an alternative to the unreliable transfers (red dot). Fig. 11 presents those transfers with a positive or negative TRO over 50,000. The blue and orange bars are the deterministic and stochastic Shapley values, respectively, with the TRO the difference between the bars. So, transfer 714–7010 has a negative TRO, implying it is an unreliable transfer, whereas transfer 766–7149 has a positive TRO, meaning that its being used as an alternative

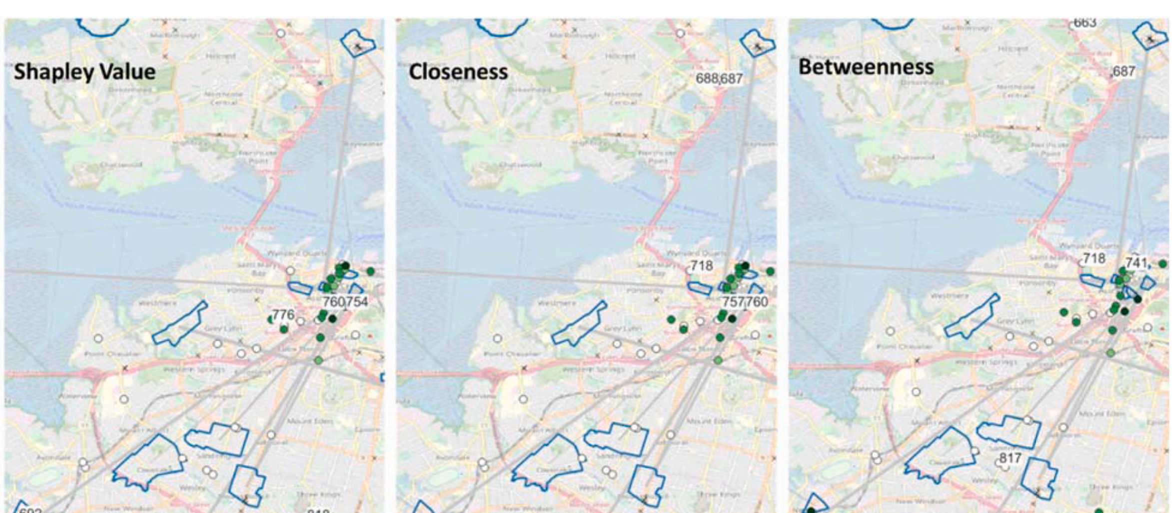

Fig. 8. The top 5 important transfers by centrality measure and location.

Table 6
Auckland PT network analysis results.

Normalized Shapley value (%)	Ideal				Deterministic				Stochastic			
	Count	Sum	Count %	Sum %	Count	Sum	Count %	Sum %	Count	Sum	Count %	Sum %
=0	73	-	44%	0%	78	-	47%	0%	78	-	47%	0%
∈ (0, 1]	49	1,182,042	29%	13%	44	1,151,094	26%	13%	43	868,523	26%	10%
∈ (1, 2]	25	3,009,043	15%	34%	25	3,014,802	15%	34%	31	3,839,453	19%	45%
∈ (2, 3]	18	3,593,124	**11%**	**41%**	18	3,562,384	**11%**	**40%**	10	2,047,166	**6%**	**24%**
∈ (3, 4]	1	308,910	**1%**	**3%**	1	317,073	**1%**	**4%**	4	1,152,451	**2%**	**13%**
∈ (4, 6]	0	-	**0%**	**0%**	0	-	**0%**	**0%**	0	-	**0%**	**0%**
>6	1	761,127	**1%**	**9%**	1	759,492	**1%**	**9%**	1	719,684	**1%**	**8%**
Total utility	167	8,854,246			167	8,804,846			167	8,627,277		
Utility reduction						49,400				177,569		

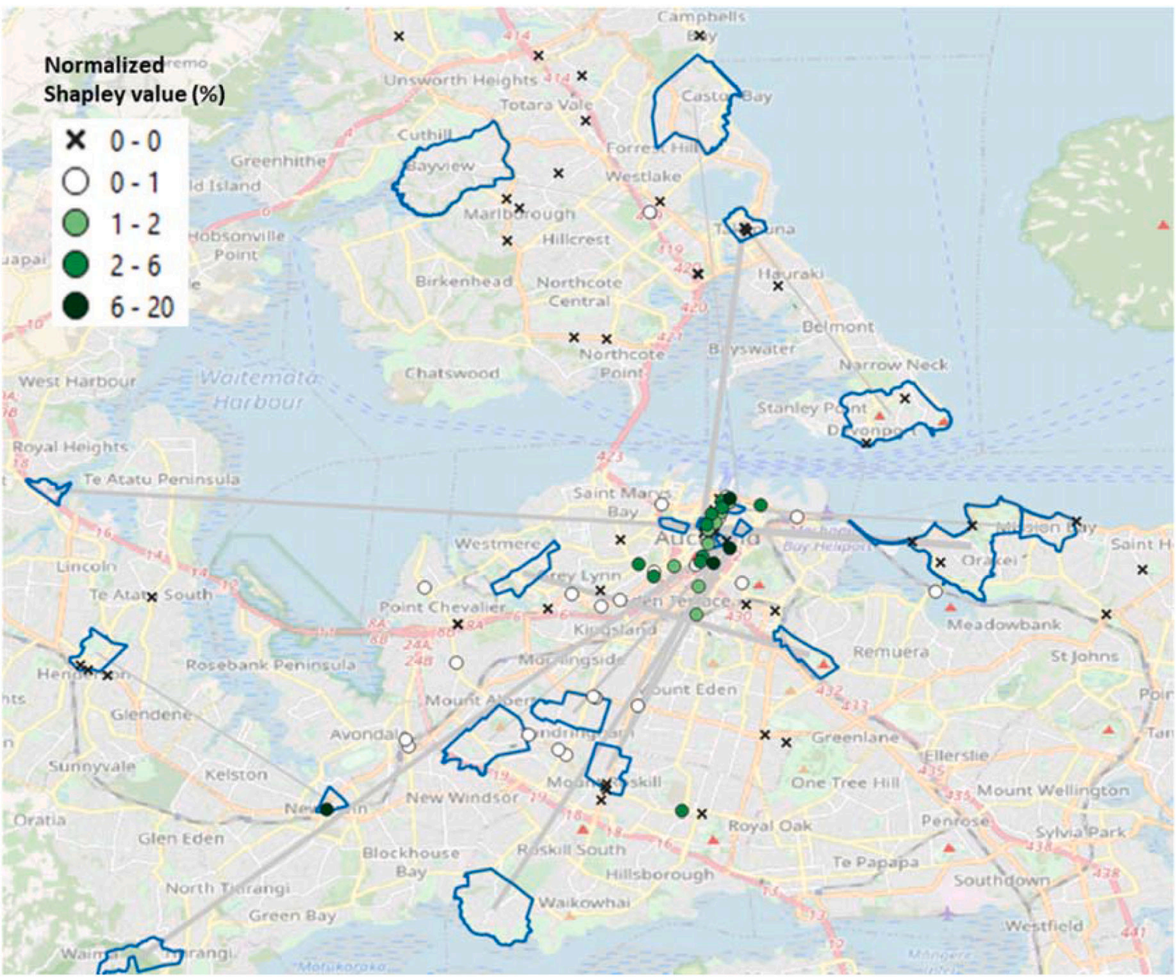

Fig. 9. The normalized Shapley value – stochastic scenario.

transfer.

Finally, considering the two indicators proposed (ORO and TRO), it is possible to identify those transfers that mostly suffer from reliability issues, as depicted in Table 7 and Fig. 12. Table 7 summarizes the positive and negative TRO, grouped by magnitude. Only 4 transfers with TRO over 50,000 (marked, bold, dark gray) contributed to 37% of the negative effect, while additional 17 (10% of all transfers) contributed additional 52% of the negative effect (marked, bold, light gray). Based on Fig. 12, which is a “zoom-in” of Fig. 10, these transfers (the red dots) can be identified and located and measures can be taken to increase their reliability.

6. Conclusions

The proposed methodology can assist the assessment and the improvement of transfers' reliability, as the two following important insights are provided by our analysis: 1) the overall decrease in the performance of the system in case of missed or delayed transfers, and 2) the identification of the transfer stops which contribute mostly to that reduction in performance.

The framework of Transportation Network (TN) cooperative games for transfer assessment in PT networks, proposed in Hadas et al. (2017), is extended into the following directions:

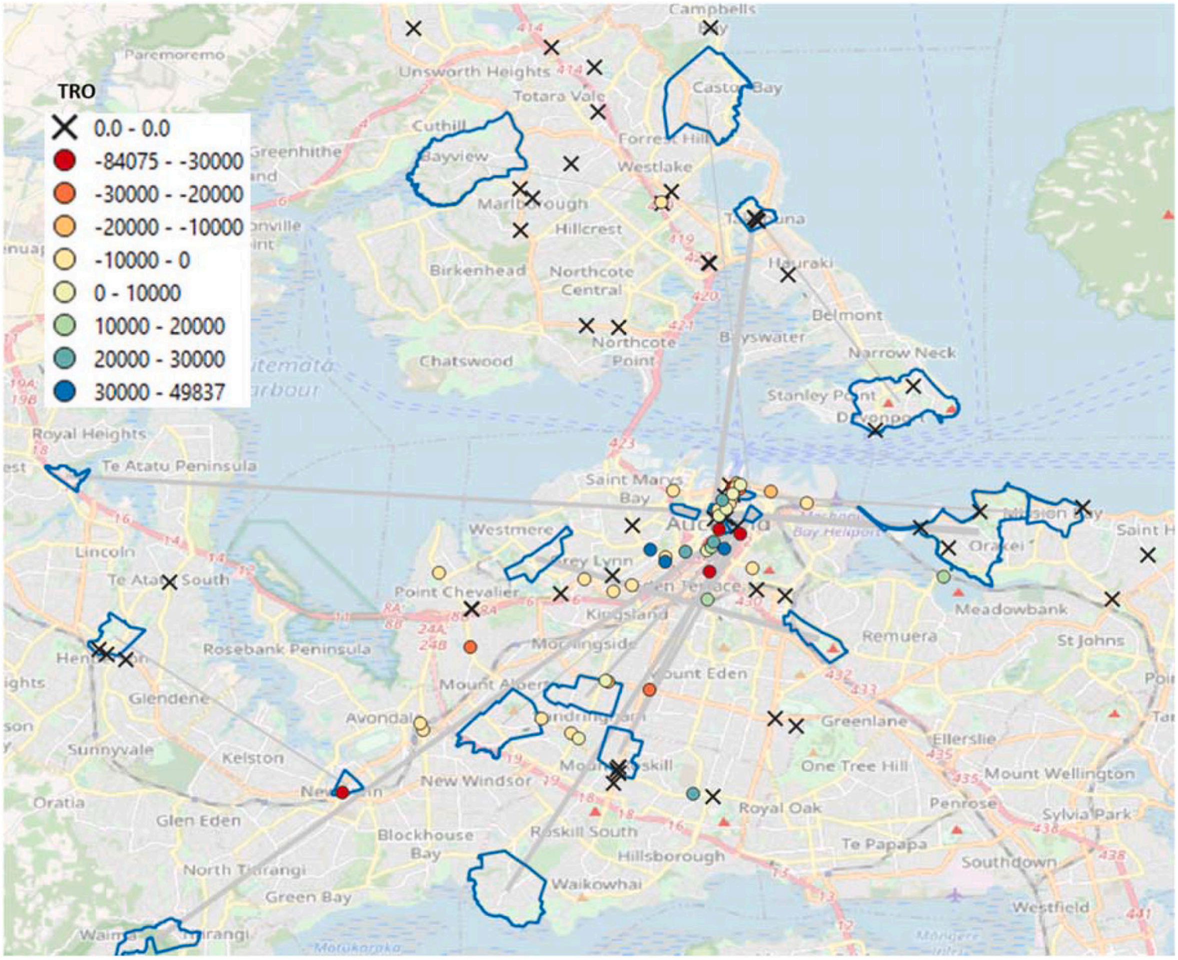

Fig. 10. The TRO between the deterministic scenario and the stochastic one.

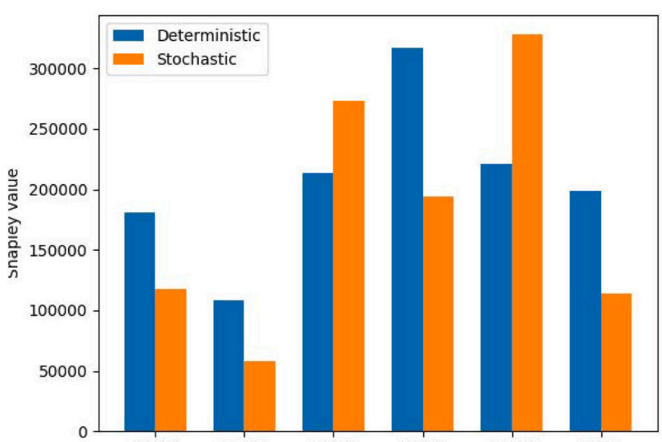

Fig. 11. Transfers with a TRO change over 50,000.

- the PT network includes stochastic arcs;
- a 2-level Monte Carlo algorithm is exploited to compute approximately the vector of Shapley values;
- a theoretical analysis of the stochastic TN cooperative game and the 2-level Monte Carlo approximation of the vector of Shapley values is made;
- a real-world scenario is used to evaluate the effectiveness of our approach.

Table 7
The distribution of TRO.

Shapley value change	Count	Sum	Count %	Sum %
−100,000	**1**	**−123,028**	**1%**	**14%**
−50,000	**3**	**−198,593**	**2%**	**23%**
−10,000	**17**	**−453,245**	**10%**	**52%**
−5000	9	−63,036	5%	7%
0	21	−31,331	13%	4%
5000	13	25,427	8%	4%
10,000	3	23,933	2%	3%
50,000	20	475,112	12%	69%
100,000	1	60,194	1%	9%
100,000+	1	106,999	1%	15%
-	78	0	47%	0%
Decrease	51	691,664		
Increase	48	−869,233		
Total	167	177,569		

Directions of future research include the incorporation of stops' sequential order within routes (Faigle and Kern, 1992), the integration of various alternatives for the players, like vehicles' frequencies (the number of trips along a route per unit of time) or vehicle size (Hsiao and Raghavan, 1993), and addressing the capacities of the road network, as well as available resources (Bell et al., 2017).

Another interesting development regards the reduction of the computational effort in the evaluation of the Shapley values, in such a way to efficiently analyze real-world networks characterized by a large number of arcs. A promising approach in this direction consists in applying supervised machine learning techniques (Shalev-Shwartz and

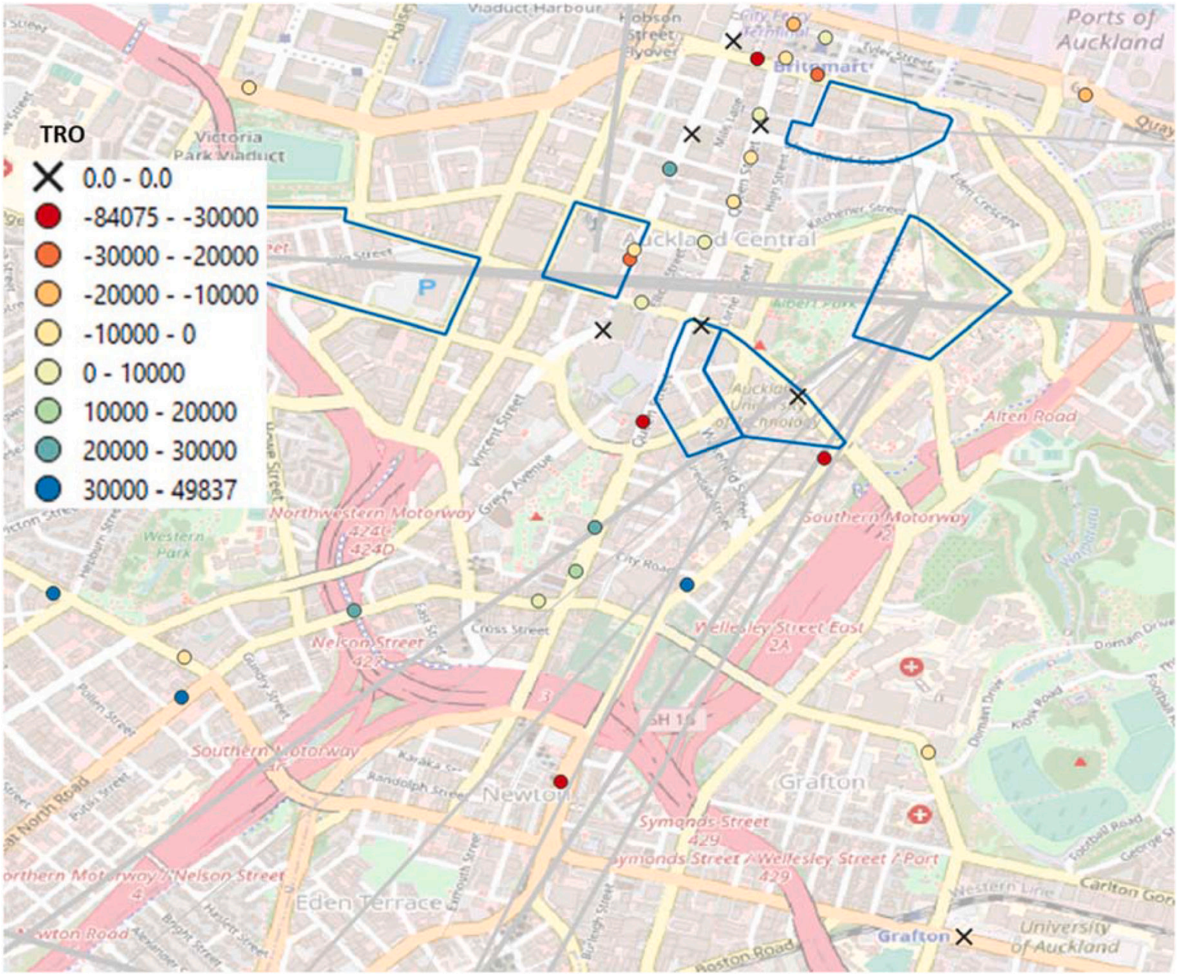

Fig. 12. City center's transfers TRO.

Ben-David, 2014) which, based on a set of supervised training pairs corresponding to a set of stochastic network models - e.g. pairs of the form [transfer times distributions, Shapley values] - allow one to estimate the Shapley values associated with other transfer times distributions.

For what concerns the algorithmic point of view, it is worth noting the connection of the stochastic TNc-ApproShapley algorithm with some classical techniques used in survey design (e.g., stratified sampling, cluster sampling; see Lehtonen and Pahkinen, 2004), which could be exploited for possible extensions of the sampling procedure. The reason for which such techniques could be useful is that the exact evaluation of the Shapley value coincides with the evaluation of an average over a "population" of permutations, and the stochastic TNc-ApproShapley algorithm just replaces such exact evaluation with a sample average.

Declaration of competing interest

The authors declare that they have no known competing financial interests or personal relationships that could have appeared to influence the work reported in this paper.

Acknowledgements

G. Gnecco and M. Sanguineti are members of GNAMPA-INdAM (Gruppo Nazionale per l'Analisi Matematica, la Probabilità e le loro Applicazioni - Istituto Nazionale di Alta Matematica). M. Sanguineti was partially supported by the Project PDGP 2018/20 DIT.AD016.001 "Technologies for Smart Communities" of INM (Institute for Marine Engineering) of CNR (National Research Council of Italy), where he is Research Associate.. He is also Affiliated Researcher at IIT - Italian Institute of Technology (Advanced Robotics Research Line), Genova, and Guest Scholar at IMT - School for Advances Studies (AXES Research Unit), Lucca.

Appendix A. Cooperative games with transferable utility (TU games) and Shapley value

A cooperative game with transferable utility (TU game) is defined as a pair (N, v), in which

$$N \; := \{1, \; \ldots, \; n\}$$

is the set of players, called grand coalition, and

$v: 2^N \rightarrow \mathbb{R}$

(where we denote by 2^N the power set of N, i.e., the set made by all its subsets) such that $v(\varnothing) = 0$ is called utility function, or characteristic function; in the following, we shall adopt the first term. The subsets $S \subseteq N$ are called (sub)coalitions. The real-valued map v assigns a utility $v(S)$ to every such coalition S. It models the utility jointly achievable by all the players belonging to S, discarding the contributions from the other players belonging to the difference set $N \backslash S$. For each player i, its utility when it does not belong to any coalition with more than one player is $v(\{i\})$.

To allocate the overall utility in a "fair way" within the set of all the players, one can exploit the Shapley value (Shapley (1953)). This defined, for each player i, as

$$Sh(i) := \sum_{S \subseteq N} \left((v(S) - v(S \backslash \{i\})) \frac{(|S|-1)!(n-|S|)!}{n!} \right)$$

in which $|S|$ indicates the number of elements of S. Intuitively, the larger the Shapley value of one player, the larger its importance. It can be proved (Tijs, 2003; González-Díaz et al., 2010) that the Shapley value of each player i represents the average marginal utility provided by i when it enters a random coalition, assuming all orders to be equally likely.

Appendix B. Transportation Network cooperative games (TNc games)

A major feature of TU games consists in the fact that the utilities can be transferred losslessly from one player to any other one. Such a property can be related to transportation networks, since when two origin-destination nodes are connected, traffic can flow between them. In the following, we provide the formulation of Transportation Network cooperative games (TNc games) for the deterministic case. Such a formulation is extended to the stochastic case in Section 2.3.

Let a PT network be modeled as either a directed or an undirected graph $G = (V, E, D, W)$, in which V and E are the sets of its nodes and of its arcs, respectively. Moreover, let D be the origin-destination matrix, which models the non-negative demand between each pair of nodes. By definition, one sets $D_{ii} := 0$ for every node i. Finally, the travel times along all the arcs of the graph are modeled by a weighted adjacency matrix W.

Now we define the (deterministic) TNc game, which is a particular instance of a TU game. In the TNc game, a coalition S is any subset of nodes of V, which induces a subgraph of G. The utility function of the game is built in the following way. For a given coalition S, first the matrix $sp(S)$ which contains the lengths of all-pair (either directed or undirected) shortest paths in the subgraph induced by S is determined. Since the goal is to evaluate a utility, whereas the weights correspond to disutilities (or costs), a suitable transformation is required. Let

$$M := \max_{S \subseteq V} \left(\max_{i,j \in S, i \neq j:\ sp(S)_{i,j} < \infty} \left(sp(S)_{i,j} \right) \right) + 1$$

be the largest (cost) diameter of any subgraph of the transportation network, plus 1. Then, for each coalition S, its utility is defined as

$$v(S) := \sum_{i,j \in S, i \neq j:\ sp(S)_{i,j} < \infty} D_{i,j} \left(M - sp(S)_{i,j} \right)$$

(if there exist no choices for $i, j \in S$ $(i \neq j)$ for which $sp(S)_{i,j} < \infty$, then one sets $v(S) := 0$). In other words, if the two nodes i and j are (directly) connected in the subgraph $G(S)$, then one can satisfy the demand between that pair of nodes and, as a consequence, the utility increases accordingly (if $D_{i,j} > 0$). Otherwise, the pair is unable to jointly contribute to the utility of the coalition S. Furthermore, the smaller the cost of a shortest path connecting a pair of nodes in the subgraph, the higher the utility. By the definition of M, $v(S)$ is always non-negative, since both $D_{i,j}$ and $M - sp(S)_{i,j}$ are non-negative.

The TNc measure of centrality is defined as the centrality measure that assigns to each node i its Shapley value in the TNc game.

Appendix C. Full results for all scenarios and transfers for the case study in Section 5

Transfer code	stop	Ideal		Deterministic			Stochastic		
		Shapley Value	Normalized Shapley value	Shapley Value	Normalized Shapley value	Difference from Ideal	Shapley Value	Normalized Shapley value	Difference from Deterministic
656	1028	10,344	0.1	7470	0.1	−2874	3433	0.0	−4037
657	1028	20,637	0.2	21,758	0.2	1121	22,874	0.3	1116
664	3362	4608	0.1	534	0.0	−4074	2	0.0	−533
665	3362	1388	0.0	549	0.0	−839	1	0.0	−548
692	5708	761,127	8.6	759,492	8.6	−1635	719,684	8.3	−39,808
696	7001	102,141	1.2	100,458	1.1	−1683	105,396	1.2	4938
697	7003	118,948	1.3	122,142	1.4	3194	122,456	1.4	314
698	7003	85,998	1.0	83,348	0.9	−2650	105,546	1.2	22,197
699	7003	68,965	0.8	71,600	0.8	2634	25,630	0.3	−45,969
700	7003	86,265	1.0	83,698	1.0	−2567	87,834	1.0	4137
701	7003	6137	0.1	5396	0.1	−740	5877	0.1	481
702	7005	176,379	2.0	172,665	2.0	−3713	154,954	1.8	−17,711
703	7005	177,179	2.0	176,414	2.0	−764	156,829	1.8	−19,585
706	7010	187,011	2.1	189,089	2.1	2078	164,913	1.9	−24,176
707	7010	195,069	2.2	188,722	2.1	−6347	202,619	2.3	13,897
708	7010	191,968	2.2	188,717	2.1	−3252	209,568	2.4	20,852
709	7010	187,892	2.1	180,785	2.1	−7107	205,901	2.4	25,115
710	7010	70,740	0.8	74,515	0.8	3775	94,281	1.1	19,766

(continued on next page)

(*continued*)

Transfer code	stop	Ideal		Deterministic			Stochastic		
		Shapley Value	Normalized Shapley value	Shapley Value	Normalized Shapley value	Difference from Ideal	Shapley Value	Normalized Shapley value	Difference from Deterministic
711	7010	190,044	2.1	192,818	2.2	2773	215,119	2.5	22,302
712	7010	119,189	1.3	117,216	1.3	−1974	119,055	1.4	1840
713	7010	188,031	2.1	187,837	2.1	−194	180,887	2.1	−6950
714	7010	188,050	2.1	181,187	2.1	−6863	117,224	1.4	−63,962
715	7018	102,234	1.2	101,863	1.2	−371	81,276	0.9	−20,587
716	7018	18,018	0.2	14,836	0.2	−3182	15,267	0.2	431
718	7037	3839	0.0	2195	0.0	−1644	6	0.0	−2189
719	7041	64,508	0.7	63,572	0.7	−936	52,592	0.6	−10,980
720	7041	9449	0.1	9410	0.1	−39	9313	0.1	−98
721	7046	27,190	0.3	25,617	0.3	−1573	21,768	0.3	−3849
722	7047	104,739	1.2	103,376	1.2	−1364	110,058	1.3	6682
723	7047	99,840	1.1	97,817	1.1	−2022	89,218	1.0	−8600
724	7047	100,991	1.1	100,702	1.1	−289	110,083	1.3	9381
726	7050	123,508	1.4	139,383	1.6	15,875	132,711	1.5	−6672
727	7051	17,245	0.2	17,573	0.2	328	13,544	0.2	−4029
728	7059	105,020	1.2	108,017	1.2	2997	99,616	1.2	−8401
729	7059	107,204	1.2	108,105	1.2	901	57,550	0.7	−50,555
730	7061	150,394	1.7	150,598	1.7	204	184,758	2.1	34,160
731	7061	48,350	0.5	51,339	0.6	2989	45,407	0.5	−5932
732	7063	108,565	1.2	108,535	1.2	−30	123,897	1.4	15,362
733	7063	112,972	1.3	114,118	1.3	1146	131,653	1.5	17,535
734	7063	108,324	1.2	104,730	1.2	−3594	127,372	1.5	22,642
735	7063	108,857	1.2	111,206	1.3	2349	68,203	0.8	−43,003
743	7079	177,746	2.0	176,564	2.0	−1182	202,550	2.3	25,987
744	7081	11,371	0.1	10,929	0.1	−443	9957	0.1	−972
745	7087	67,031	0.8	62,918	0.7	−4113	65,514	0.8	2596
746	7087	187,916	2.1	186,732	2.1	−1184	160,930	1.9	−25,801
748	7094	148,158	1.7	148,223	1.7	65	148,316	1.7	93
749	7131	6031	0.1	6675	0.1	645	9041	0.1	2366
750	7131	6210	0.1	6275	0.1	65	5795	0.1	−480
751	7135	66,852	0.8	68,737	0.8	1885	90,964	1.1	22,227
752	7147	9485	0.1	9861	0.1	376	13,412	0.2	3551
753	7147	24,316	0.3	24,302	0.3	−14	2869	0.0	−21,433
754	7147	246,217	2.8	244,285	2.8	−1932	283,639	3.3	39,353
755	7147	32,547	0.4	31,644	0.4	−903	19,787	0.2	−11,857
756	7147	129,252	1.5	129,685	1.5	433	148,712	1.7	19,027
757	7147	142,403	1.6	138,279	1.6	−4124	137,915	1.6	−364
758	7147	132,075	1.5	129,397	1.5	−2678	87,797	1.0	−41,599
759	7147	213,664	2.4	213,376	2.4	−288	273,570	3.2	60,194
760	7147	308,910	3.5	317,073	3.6	8163	194,045	2.2	−123,028
762	7149	9091	0.1	8937	0.1	−154	526	0.0	−8410
763	7149	130,613	1.5	128,823	1.5	−1790	154,836	1.8	26,013
764	7149	137,280	1.6	135,455	1.5	−1825	101,487	1.2	−33,968
765	7149	112,352	1.3	117,228	1.3	4875	116,832	1.4	−395
766	7149	221,562	2.5	221,016	2.5	−546	328,015	3.8	106,999
767	7149	213,828	2.4	211,555	2.4	−2273	171,154	2.0	−40,401
769	7151	201,061	2.3	198,370	2.3	−2692	114,294	1.3	−84,075
774	7211	9533	0.1	9360	0.1	−173	8584	0.1	−776
775	7211	17,464	0.2	14,721	0.2	−2743	9364	0.1	−5357
776	7214	226,111	2.6	224,114	2.5	−1997	267,227	3.1	43,113
778	7305	5818	0.1	5077	0.1	−741	4768	0.1	−310
782	7769	72,277	0.8	68,256	0.8	−4021	84,440	1.0	16,184
787	8011	12,191	0.1	11,958	0.1	−234	8479	0.1	−3478
788	8047	19,662	0.2	18,978	0.2	−684	1980	0.0	−16,998
789	8048	19,085	0.2	18,605	0.2	−480	21,301	0.2	2696
790	8052	13,430	0.2	12,875	0.1	−555	8483	0.1	−4392
791	8052	24,900	0.3	23,071	0.3	−1830	5298	0.1	−17,773
793	8101	184,694	2.1	181,802	2.1	−2892	219,845	2.5	38,044
794	8109	41,252	0.5	42,536	0.5	1284	36,500	0.4	−6036
795	8111	19,517	0.2	19,152	0.2	−365	18,878	0.2	−273
796	8117	12,269	0.1	10,471	0.1	−1798	9858	0.1	−613
803	8331	20,859	0.2	20,371	0.2	−488	20,117	0.2	−254
808	8503	114,477	1.3	116,712	1.3	2234	135,178	1.6	18,466
809	8534	20,559	0.2	20,097	0.2	−462	13,419	0.2	−6678
812	8826	21,361	0.2	19,802	0.2	−1560	20,670	0.2	868
813	8826	10,007	0.1	11,325	0.1	1318	10,567	0.1	−758
814	8827	9770	0.1	9772	0.1	2	8285	0.1	−1487
817	8833	26,146	0.3	26,508	0.3	362	25,012	0.3	−1496
818	8842	215,080	2.4	219,004	2.5	3923	231,872	2.7	12,869
819	8842	113,130	1.3	110,072	1.3	−3057	117,942	1.4	7869
820	8879	23,761	0.3	24,471	0.3	710	2875	0.0	−21,596

Appendix D. Proofs

Proof of Proposition 1. For each realization of the graph (V,E,D,W,P^1,P^2), each ordered pair of nodes (i,j) which belongs to the set $S^{'}$ associated with the coalition S provides to the utility $v^{'}(S^{'})$ a contribution $D_{i,j}(M - sp(S'_k)_{i,j})$ in case the nodes belong to the same connected component of $G(S^{'})$, otherwise the contribution is 0. Thus, one gets

$$E\{v^{'}(S^{'})\} = E\left\{\sum_{i,j\in S^{'},i\neq j, sp(S^{'})_{i,j}<\infty} D_{i,j}(M - sp(S^{'})_{i,j})\right\} = E\left\{\sum_{k=1}^{C_{S^{'}}}\sum_{i,j\in S'_k, i\neq j} D_{i,j}(M - sp(S'_k)_{i,j})\right\} \blacksquare$$

Proof of. Proposition 2Monotonicity follows by the definition of the utility function v in equation (2): for each realization of the set of stochastic arcs, if a path is present in the subgraph induced by $S^{'}$, then it is also present in the subgraph induced by $T^{'}$, with smaller or equal cost. Hence, one gets

$$E\left\{\sum_{i,j\in T^{'},i\neq j:\ sp(T^{'})_{i,j}<\infty} D_{i,j}(M - sp(T^{'})_{i,j})\right\} \geq E\left\{\sum_{i,j\in S^{'},i\neq j:\ sp(S^{'})_{i,j}<\infty} D_{i,j}(M - sp(S^{'})_{i,j})\right\} \blacksquare$$

Proof of Proposition 3. The statement is proved by combining

- the interpretation of the Shapley value of each player i as the average marginal contribution provided by that player to any coalition, by taking into account all possible coalitional scenarios and assuming that all the orders of players entering the coalitions are equally likely (Tijs, 2003; González-Díaz et al., 2010);
- the independence of the mechanisms according to which the random permutation and the stochastic arcs are sampled in the stochastic TNc-ApproShapley algorithm. $\blacksquare$

Proof of Proposition 4 (i). Likewise in Ryan (2003), one can analyze the variance (6) of the approximation $Sh^{'}(i)$ by applying the law of total variance. This expresses the variance of a random variable Y as the sum of the variance of its conditional expectation (conditioned on another set of random variables $X_1,...,X_s$), and the expectation of its conditional variance (conditioned on the same set of random variables $X_1,...,X_s$):

$$\mathrm{var}\{Y\} = \mathrm{var}\{E\{Y|X_1,...,X_s\}\} + E\{\mathrm{var}\{Y|X_1,...,X_s\}\}$$

It is worth observing that both $E\{Y|X_1,...,X_s\}$ and $\mathrm{var}\{Y|X_1,...,X_s\}$ are random variables. In our specific case, for every player i, the equation above can be applied by taking $Y = Sh^{'}(i)$ and being $X_1,...,X_s$ a total of S_P independent samples of the random permutation (which are denoted by $m_1,...,m_{S_P}$). Then, starting from the decomposition of $\mathrm{var}\{Y\}$, one obtains the next expression for the variance of the approximation $Sh^{'}(i)$:

$$\mathrm{var}\{Sh^{'}(i)\} = \mathrm{var}\{E\{Sh^{'}(i)|m_1,...,m_{S_P}\}\} + E\{\mathrm{var}\{Sh^{'}(i)|m_1,...,m_{S_P}\}\}$$

By adopting an argument similar to the one made in Section 3 of Ryan (2003) it can be seen that, by the assumed independence of the S_P random permutations, the expression above of $\mathrm{var}\{Sh^{'}(i)\}$ can be also written as

$$\mathrm{var}\{Sh^{'}(i)\} = \frac{1}{S_P}(\mathrm{var}\{E\{Sh^{'}(i)|m_1\}\} + E\{\mathrm{var}\{Sh^{'}(i)|m_1\}\})$$

Conditioned on m_1, $Sh^{'}(i)$ is the empirical average of a total of N_R independent samples having the same variance, and being drawn from the same distribution. Hence,

$$\mathrm{var}\{Sh^{'}(i)|m_1\} = \frac{1}{N_R}\mathrm{var}\{Sh^{'}(i)|m_1\}|_{1\ \text{realization}}$$

where $\mathrm{var}\{Sh^{'}(i)|m_1\}|_{1\ \text{realization}}$ relates to the particular case $N_R = 1$. By taking into account both previous equations, one gets

$$\mathrm{var}\{Sh^{'}(i)\} \leq \frac{A}{S_P} + \frac{B}{S_P N_R}$$

where $A = \mathrm{var}\{E\{Sh^{'}(i)|m_1\}\} \geq 0$, and $B = E\{\mathrm{var}\{Sh^{'}(i)|m_1\}|_{1\ \text{realization}}\} \geq 0$. $\blacksquare$

Proof of Proposition 4 (ii). The random variables $E\{Sh^{'}(i)|m_1\}$ and $Sh^{'}(i)|m_1|_{1\ \text{realization}}$ in the definitions of A and B are both bounded from below by 0, and from above by the maximum realization $v'_{max}(N)$ of the random utility $v^{'}(N)$ of the grand coalition, whose expression depends on the specific stochastic TNc game. Hence, they are both bounded random variables. By applying Popoviciu's inequality (Popoviciu, 1935), one gets

$$A = \mathrm{var}\{E\{Sh^{'}(i)|m_1\}\} \leq \frac{v^{'}_{\max}(N)}{2}$$

and

$$B = E\left\{\mathrm{var}\{Sh^{'}(i)|m_1\}|_{1\ \text{realization}}\right\} \leq \frac{v^{'}_{\max}(N)}{2}$$

Hence, by Proposition 4 (i) one obtains

$$\mathrm{var}\{Sh^{'}(i)\} \leq \frac{v^{'}_{\max}(N)}{2} + \frac{v^{'}_{\max}(N)}{2S_P N_R} = \frac{v^{'}_{\max}(N)}{2}\cdot\frac{N_R+1}{S_P N_R} \blacksquare$$

References

Ahuja, R.K., Magnanti, T.L., Orlin, J.B., 1993. Network Flows: Theory, Algorithms, and Applications. Prentice Hall, Englewood Cliffs, N.J.

Bates, J., Polak, J., Jones, P., et al., 2001. The valuation of reliability for personal travel. Transport. Res. E Logist. Transport. Rev. 37 (2), 191–229.

Bell, M.G.H., 2000. A game theory approach to measuring the performance reliability of transport networks. Transp. Res. Part B Methodol. 34 (6), 533–545.

Bell, M.G.H., Kurauchi, F., Perera, S., et al., 2017. Investigating transport network vulnerability by capacity weighted spectral analysis. Transp. Res. Part B Methodol. 99, 251–266.

Black, W.R., 2003. Transportation: a Geographical Analysis. Guilford Press, New York.

Bombelli, A., Santos, B.F., Tavasszy, L., 2020. Analysis of the air cargo transport network using a complex network theory perspective. Transport. Res. E Logist. Transport. Rev. 138, 101959.

Castro, J., Gómez, D., Tejada, J., 2009. Polynomial calculation of the Shapley value based on sampling. Comput. Oper. Res. 36 (5), 1726–1730.

Chen, X., Yu, L., Zhang, Y., et al., 2009. Analyzing urban bus service reliability at the stop, route, and network levels. Transport. Res. Pol. Pract. 43 (8), 722–734.

Cheung, K.-F., Bell, M.G., Pan, J.-J., et al., 2020. An eigenvector centrality analysis of world container shipping network connectivity. Transport. Res. E Logist. Transport. Rev. 140, 101991.

Cokelaer, T., 2019. Fitter - Python distribution fitter package. Available at: https://fitter.readthedocs.io/en/latest/.

Faigle, U., Kern, W., 1992. The Shapley value for cooperative games under precedence constraints. Int. J. Game Theor. 21 (3), 249–266.

Gnecco, G., Hadas, Y., Sanguineti, M., 2019. Some properties of transportation network cooperative games. Networks 74 (2), 161–173.

Gnecco, G., Hadas, Y., Sanguineti, M., 2021. Public transport transfers assessment via transferable utility games and Shapley value approximation. Transportmetrica: Transport. Sci. 17 (4), 540–565.

González-Díaz, J., García-Jurado, I., Fiestras-Janeiro, M.G., 2010. An Introductory Course on Mathematical Game Theory. American Mathematical Society Providence.

Google Transit, 2010. Google transit. Available at: http://maps.google.com/intl/en/landing/transit/#mdy. (Accessed 10 June 2010). accessed.

Gu, Y., Fu, X., Liu, Z., et al., 2020. Performance of transportation network under perturbations: reliability, vulnerability, and resilience. Transport. Res. E Logist. Transport. Rev. 133, 101809.

Hadas, Y., 2013. Assessing public transport systems connectivity based on Google Transit data. J. Transport Geogr. 33, 105–116.

Hadas, Y., Ceder, A., 2010. Optimal coordination of public-transit vehicles using operational tactics examined by simulation. Transport. Res. Part C 18 (6), 879–895.

Hadas, Y., Gnecco, G., Sanguineti, M., 2017. An approach to transportation network analysis via transferable utility games. Transp. Res. Part B Methodol. 105, 120–143.

Hadas, Y., Gnecco, G., Sanguineti, M., 2018. Public transport transfers assessment via transferable-utility games and shapley-value approximation. In: 97th Annual Meeting of the Transportation Research Board. Transportation Research Board of the National Academies, Washington D.C.

Hadas, Y., Ranjitkar, P., 2012. Modeling public-transit connectivity with spatial quality-of-transfer measurements. J. Transport Geogr. 22, 137–147.

Hsiao, C.-R., Raghavan, T., 1993. Shapley value for multichoice cooperative games, I. Game. Econ. Behav. 5 (2), 240–256.

Jenelius, E., Mattsson, L.-G., 2015. Road network vulnerability analysis: conceptualization, implementation and application. Comput. Environ. Urban Syst. 49, 136–147.

Lehtonen, R., Pahkinen, E., 2004. Practical Methods for Design and Analysis of Complex Surveys. John Wiley & Sons.

Li, X., Rey, D., Dixit, V.V., 2018. An axiomatic characterization of fairness in transport networks: application to road pricing and spatial equity. Transport Pol. 68, 142–157.

Lin, C.-C., Hsieh, C.-C., 2012. A cooperative coalitional game in duopolistic supply-chain competition. Network. Spatial Econ. 12 (1), 129–146.

Mees, P., 2010. Transport for Suburbia : beyond the Automobile Age. Earthscan, London; Sterling, VA.

Mishra, S., Welch, T.F., Jha, M.K., 2012. Performance indicators for public transit connectivity in multi-modal transportation networks. Transport. Res. Pol. Pract. 46 (7), 1066–1085.

Moritz, P., Nishihara, R., Wang, S., et al., 2018. Ray: a distributed framework for emerging AI applications. Proc. 13th USENIX Symposium on Operating Systems Design and Implementation (OSDI '18) 561–577. October 8–10, 2018 , Carlsbad, CA, USA.

Narayanam, R., Narahari, Y., 2011. A Shapley value-based approach to discover influential nodes in social networks. IEEE Trans. Autom. Sci. Eng. 8 (1), 130–147.

Nesheli, M.M., Ceder, A., 2015. Improved reliability of public transportation using real-time transfer synchronization. Transport. Res. C Emerg. Technol. 60, 525–539.

Nielsen, G., Nelson, J.D., Mulley, C., et al., 2005. HiTrans Best Practice Guide 2 - Public Transport – Planning the Networks. Stavanger, Norway. HiTrans, 2005.

OpenStreetMap, 2012. OpenStreetMap foundation. Available at: http://wiki.osmfoundation.org/wiki/Main_Page. (Accessed 22 May 2013).

OpenTripPlanner, 2020. Multimodal trip planning. Available at: http://www.opentripplanner.org/.

Pedregosa, F., Varoquaux, G., Gramfort, A., et al., 2011. Scikit-learn: machine learning in Python. J. Mach. Learn. Res. 12, 2825–2830.

Popoviciu, T., 1935. Sur les équations algébriques ayant toutes leurs racines réelles. Mathematica 9, 129–145.

Redman, L., Friman, M., Gärling, T., et al., 2013. Quality attributes of public transport that attract car users: a research review. Transport Pol. 25, 119–127.

Reggiani, A., Nijkamp, P., Lanzi, D., 2015. Transport resilience and vulnerability: the role of connectivity. Transport. Res. Pol. Pract. 81, 4–15.

Rodrigue, J.-P., Comtois, C., Slack, B., 2006. The Geography of Transport Systems. Routledge, Abingdon, Oxon, England; New York.

Roson, R., Hubert, F., 2015. Bargaining power and value sharing in distribution networks: a cooperative game theory approach. Network. Spatial Econ. 15 (1), 71–87.

Ryan, K.J., 2003. Estimating expected information gains for experimental designs with application to the random fatigue-limit model. J. Comput. Graph Stat. 12 (3), 585–603.

Shalev-Shwartz, S., Ben-David, S., 2014. Understanding Machine Learning: from Theory to Algorithms. Cambridge University Press.

Shapley, L.S., 1953. A value for N-person games. In: Kuhn, H.W., Tucker, A.W. (Eds.), Contributions to the Theory of Games. Princeton University Press, New Jersey, pp. 307–318.

Tijs, S.H., 2003. Introduction to Game Theory. Hindustan Book Agency.

van den Nouweland, A., Slikker, M., 2001. Social and Economic Networks in Cooperative Game Theory. Kluwer Academic Publishers, Boston.

Wasserman, S., Faust, K., 1994. Social Network Analysis: Methods and Applications. Cambridge University Press.

Wilson, N.M., Zhao, J., Rahbee, A., 2009. The potential impact of automated data collection systems on urban public transport planning. In: Wilson, N.H.M., Nuzzolo, A. (Eds.), Schedule-Based Modeling of Transportation Networks. Springer, USA, pp. 1–25.

Yao, B., Hu, P., Lu, X., et al., 2014. Transit network design based on travel time reliability. Transport. Res. C Emerg. Technol. 43, 233–248.